Inorg. Chem. **2004**, *43*, 3349–3370

Photoelectron Spectroscopic and Electronic Structure Studies of CH_2O Bonding and Reactivity on ZnO Surfaces: Steps in the Methanol Synthesis Reaction

P. M. Jones, J. A. May, J. B. Reitz, and Edward I. Solomon*

Department of Chemistry, Stanford University, Stanford, California 94305

Received October 29, 2003

Adsorption of CH_2O on ZnO**(0001)** has been investigated using XPS, NEXAFS, variable-energy photoelectron spectroscopy (PES), and density functional theory (DFT) calculations. CH_2O is chemisorbed on the **(0001)** surface at 130 K. Its C1s XPS peak position at 292.7 eV and NEXAFS σ^* shape resonance at 302.6 eV are consistent with an η^1 bound surface geometry. Geometry optimized DFT calculations also indicate that CH_2O is bound to the Zn(II) site in an η^1 configuration through its oxygen atom. The variable-energy PES of the η^1 bound CH_2O/ZnO-**(0001)** complex exhibits four valence band features at 21.2, 16.4, 13.8, and 10.7 eV below the vacuum level providing an experimental and theoretical description of this surface interaction. Annealing the ZnO**(0001)**/CH_2O surface complex to 220 K decomposes the chemisorbed CH_2O, producing formyl (291.5 eV), methoxide (290.2 eV), and formate (293.6 eV) intermediates. Thus this reaction coordinate involves the conversion of an oxygen bound formaldehyde to a carbon bound formyl species on ZnO**(0001)**. Only formate is formed on the ZnO**(10$\bar{1}$0)** surface. DFT is used to explore surface intermediates and the transition state in the methanol synthesis reaction (MSR). The bonding interactions of H_2, CO, CH_3O^-, HCO^-, and *trans*-HCOH to the ZnO**(0001)** surface are elucidated using geometry optimization. H_2 was found to be heterolytically cleaved on the ZnO**(0001)** surface, and carbon monoxide, formyl, and methoxide are calculated to be η^1 bound. These results are consistent with observed metal oxide surface reactivity where heterolytic bond cleavage is dominant. The oxygen atom in the bound formyl was found to be activated for attack by a proton. This results in the planar η^1 bound *trans*-HCOH surface species. The transition state in the gas phase rearrangement of *trans*-HCOH to formaldehyde was calculated to have a barrier of 31 kcal/mol. The correlation diagram for this rearrangement in the gas phase indicates that configuration interaction at the crossing of two levels helps to lower the barrier. A transition state calculation was also performed for this rearrangement on the ZnO**(0001)** surface. The surface transition state geometry is significantly different than the gas phase. The surface geometry is no longer planar (23° dihedral angle) and is displaced parallel to the surface. Interaction with the Zn(II) site at the crossing of surface bound CH_2O and *trans*-HCOH levels further lowers the barrier to rearrangement relative to gas phase by 9 kcal/mol. The rearrangement of *trans*-HCOH (carbon bound) to CH_2O (oxygen bound) on ZnO**(0001)** was calculated to be the overall barrier of the MSR reaction.

1. Introduction

The modern form of the methanol synthesis reaction (MSR) shown in eq 1 is catalyzed at low temperature (473−523 K) and pressures (50−100 atm) by the Cu/ZnO binary catalyst.[1,2] Before the availability of the binary catalyst, ZnO was used at higher reaction temperatures and pressures, where the addition of copper to the ZnO catalyst reduces the activation barrier for this reaction (from approximately 30 kcal/mol to 18 kcal/mol).

$$CO + 2H_2 \xrightarrow{Cu/ZnO} CH_3OH \qquad (1)$$

Due to its industrial importance the binary catalyst has been extensively studied. Klier et al. have shown that it contains a high affinity CO binding site that correlates with catalyst activity.[3−8] Didzulis et al.[9] have shown that substitutional Cu(I) C_{3v} sites are the high affinity CO binding sites.

* Author to whom correspondence should be addressed. E-mail: edward.solomon@stanford.edu.

(1) Lee, S. *Methanol Synthesis Technology*; CRC Press: Boca Raton, FL, 1990.
(2) Cheng, W. H., Kung, H. H., Cheng, W. H., Kung, H. H., Eds. Marcel Dekker: New York, 1994; pp 1−22.

10.1021/ic035252q CCC: $27.50
Published on Web 05/05/2004

In contrast, the ICI group has shown that the activity of the industrial catalyst also correlates with the surface area of dispersed copper metal on the ZnO surface.[10−13]

CO_2 is typically added to the feedstock over the binary catalyst[1]. Radio-labeling experiments have shown that, under the conditions of the study, methanol is formed from CO_2 and not CO[14] (eq 2).

$$CO_2 + 3H_2 \xrightarrow{Cu/ZnO} CH_3OH + H_2O \quad (2)$$

The binary catalyst is also a highly effective water−gas shift catalyst (eq 3), thereby complicating this result.[15,16]

$$H_2O + CO \xrightarrow{Cu/ZnO} CO_2 + H_2 \quad (3)$$

Unlike the binary catalyst, ZnO is ineffective as a water−gas shift catalyst;[17,18] furthermore, the addition of increasing amounts of CO_2 to the feedstock over ZnO dramatically reduces the effectiveness of this catalyst.[1] Early chemical trapping experiments and FT-IR studies have indicated the presence of formyl as a reaction intermediate in the MSR over ZnO, providing support for the sequential hydrogenation of surface bound CO as the principal route to the formation of methanol over ZnO. Therefore, when compared to the binary catalyst ZnO provides a more direct (no water−gas shift) and simpler (only CO forms methanol) surface system in which to study the molecular basis of this catalysis.

ZnO is a classic coordination compound (or Werner) surface, which provides access to interesting surface chemistry and unique spectral features when compared to metallic surfaces. ZnO has been shown to heterolytically cleave H_2 forming a hydride (H^-) and a hydroxide (H^+) and readily deprotonates methanol to form methoxide (CH_3O^-). In contrast, on metallic surfaces, these adsorbates yield a surface hydrogen atom with some hydride character and methoxy ($CH_3O^\bullet$) species, respectively. These products emphasize the important reactivity differences between these surfaces.

ZnO has a wurtzite structure. The polar ZnO**(0001)** surface contains an outermost layer of coordinatively unsaturated Zn(II) sites with a next nearest layer of oxide anions, exposing both Lewis acid and Bronsted base sites. The ZnO**(10$\bar{1}$0)** surface is nonpolar containing pairs of coordinatively unsaturated Zn(II) and oxide sites.[19,20] The direction of unsaturation of Zn(II) on this surface is tilted at 19° from the surface normal.[21,22]

These ZnO surfaces have been extensively used to study the adsorption and surface chemistry of small molecules relevant to the MSR. The elucidation of the surface bond of CO and methanol is of particular importance in the understanding of the MSR over ZnO. Previous studies in this laboratory using PES, NEXAFS, and electronic structure calculations have revealed that bound surface species are in η^1 geometry.[23] Carbon monoxide is bound through its carbon atom and is activated for attack by a net positive charge at this atom. Methanol was found to be deprotonated on the ZnO surface forming the surface bound methoxide.[24] This result is in agreement with an earlier theoretical study of Baetzold[25] which indicated that methoxide, and not hydroxymethyl, is stabilized on the Zn(II) site. Thus the Costa−Meutterties (CM) reaction scheme was developed, which begins with surface bound CO and yields the oxygen bound methoxide.[26−28] The reaction of methanol with the different ZnO surfaces was found to yield different chemical species. The surface dependent formation of a formaldehyde intermediate from methoxide was proposed to be a necessary step to its further decomposition to formate on the **(0001)** surface.[24] Kung et al.[29,30] have used single crystal surfaces of ZnO to probe the decomposition of CH_3OH with TPD; they showed that the ZnO**(0001)** is the dominate surface for this reaction where the main decomposition product was CO under the conditions of their experiment.

Prior theoretical studies have sought to establish the bonding geometry, electronic structure, and surface chemistry of the experimentally observed intermediates. In a series of papers Casarin et al.[31,32] have utilized density functional theory (DFT) and geometry optimization on large ZnO cluster models of the crystal surfaces to establish the surface geometry and binding energy of several of the important

(3) Bulko, J. B.; Herman, R. G.; Klier, K.; Simmons, G. W. *J. Phys. Chem* **1979**, *83*, 3118.
(4) Dominquez, J. M.; Simmons, G. W.; Klier, K. *J. Mol. Catal.* **1983**, *20*, 369.
(5) Klier, K. *Adv. Catal.* **1982**, *31*, 243.
(6) Herman, R. G.; Klier, K.; Simmons, G. W.; Fin, B. P.; Bulko, J. B.; Kobylinski, T. P. *J. Catal.* **1979**, *56*, 407.
(7) Mehta, S.; Simmons, G. W.; Klier, K.; Herman, R. G. *J. Catal.* **1979**, *57*, 343.
(8) Klier, K.; Chatikavanij, V.; Herman, R. G.; Simmons, G. W. *J. Catal.* **1982**, *74*, 343.
(9) Didziulis, S. V.; Butcher, K. D.; Cohen, S. L.; Solomon, E. I. *J. Am. Chem. Soc.* **1989**, *111*, 7110.
(10) Denise, B.; Sneeden, R. P. A.; Beguin, B.; Cherifi, O. *Appl. Catal.* **1987**, *30*, 353.
(11) Chinchen, G. C.; Waugh, K. C.; Whan, D. A. *Appl. Catal.* **1986**, *25*, 101.
(12) Chinchen, G. C.; Waugh, J. C. *J. Catal.* **1986**, *97*, 280.
(13) Chinchen, G. C.; Mansfield, K.; Spencer, M. S. *CHEMTECH* **1990**, *20*, 692.
(14) Kagan, Y. B.; Rozovskii, A. Y.; Lin, G. I.; Slivinskii, E. V.; Loktev, S. M.; Liberov, L. G.; Bashkirov, A. N. *Kinet. Katal.* **1975**, *16*, 704.
(15) Satterfield, C. N. *Heterogeneous Catalysis In Practice*; McGraw-Hill: New York, 1980.
(16) Ren, Z. X.; Wang, J.; Jia, L. J.; Lu, D. S. *Appl. Catal.* **1989**, *49*, 83−90.
(17) Kung, H. H. *Transition Metal Oxides: Surface Chemistry and Catalysis*; Elsevier Science Publishers: New York, 1989; Vol. 45.
(18) Rethwisch, D. G.; Dumesic, J. A. *Langmuir* **1986**, *2*, 73−79.
(19) Gay, R. R.; Nodine, M. H.; Henrich, V. E.; Zeiger, H. J.; Solomon, E. I. *J. Am. Chem. Soc.* **1980**, *102*, 6752.
(20) Abrahams, S. C.; Bernstein, J. L. *Acta Crystallogr, Sect. B* **1969**, *b25*, 1233.
(21) Duke, C. B.; Meyer, R. J.; Paton, A.; Mark, P. *Phys. Rev. B* **1978**, *18*, 4225.
(22) D'Amico, K. L.; Trenary, M.; Shinn, N. D.; Solomon, E. I.; McFeely, F. R. *J. Am. Chem. Soc.* **1982**, *104*, 5102.
(23) Lin, J.; Jones, P.; Guckert, J.; Solomon, E. I. *J. Am. Chem. Soc.* **1991**, *113*, 8312.
(24) Jones, P. M.; May, J. A.; Reitz, J. B.; Solomon, E. I. *J. Am. Chem. Soc* **1998**, *120*, 1506−1516.
(25) Baetzold, R. C. *J. Phys. Chem.* **1985**, *89*, 4150.
(26) Costa, L. C. *Catal. Rev.−Sci. Eng.* **1983**, *25*, 325.
(27) Fahey, D. R. *J. Am. Chem. Soc.* **1981**, *103*, 136.
(28) Muetterties, E. L.; Stein, J. *J. Chem. Soc. Rev.* **1979**, *79*, 479.
(29) Cheng, W. H.; Akhter, S.; Kung, H. H. *J. Catal.* **1983**, *82*, 341−350.
(30) Akhter, S.; Lui, K.; Kung, H. H. *J. Phys. Chem.* **1985**, *89*, 1958−1964.
(31) Casarin, M.; Tondello, E.; Vittadini, A. *Surf. Sci.* **1994**, *303*, 125−138.
(32) Casarin, M.; Tondello, E.; Vittadini, A. *Inorg. Chim. Acta* **1995**, *235*, 151−158.

MSR intermediates. These researchers have calculated that CO donates charge to the Zn(II) bonding site, thereby contracting the C−O bond and shifting its stretching frequency to higher energy. These results are consistent with previous experimental studies. Prior studies in this laboratory using experiment and Xα-SW calculations[33] have probed the electronic structure of the Zn(II)−CO bond, revealing it to be dominated by the CO 5σ donor interaction with the Zn 4s and 4p. A subsequent study, using the same methods, on the interaction of methoxide with ZnO**(0001)** has shown that the σ_O and π_{CO} molecular orbitals of the chemisorbed methoxide interact with the Zn 4s and 4p levels to form the methoxide donor surface bond.[24]

The methanol synthesis reaction over ZnO, starting with CO, has been thought to proceed via a hydride transfer forming the formyl anion.[26−28] The next step, in this reaction scheme, is likely the formation of formaldehyde or its isomer, *trans*-HCOH. The formation of formaldehyde from H_2 and CO in the gas phase is thermodynamically uphill.[34] The H_2−CO gas phase interaction has been the subject of numerous theoretical studies.[35−38] In particular, it has been found that the rearrangement of hydroxymethylene (HCOH) to formaldehyde takes place with a large barrier. To our knowledge no studies exist that probe this rearrangement on a surface. According to the CM reaction scheme, once the surface bound formaldehyde is formed, it abstracts a hydride to form the surface bound methoxide. On the ZnO surface this entire reaction takes place with an experimental barrier of ∼30 kcal/mol. The origins of this barrier in the gas phase and how it changes on the surface are central goals of the present study.

This study extends our previous studies of CO and CH_3O^- bonding on ZnO by systematically applying electron spectroscopies and DFT calculations to the bonding and reactivity of formaldehyde on single crystal zinc oxide (**(0001)** and **(10$\bar{1}$0)**) surfaces. It probes, in a stepwise manner, the bonding of H_2, CO, HCO^- and the rearrangement of hydroxymethylene to formaldehyde on the surface using experimentally calibrated geometry optimized DFT and transition state calculations on the ZnO surface, defining the MSR reaction coordinate and providing electronic structure insight into the barrier of this reaction.

The XPS and NEXAFS of low temperature and low coverage formaldehyde on the ZnO**(0001)** surface are presented in sections 3.1.1 and 3.1.2, respectively. The variable energy PES of formaldehyde on ZnO**(0001)** (section 3.1.3**)** is correlated with the calculated geometric and electronic structure of the optimized surface bound CH_2O in sections 3.2.1 and 3.2.2, respectively. Formaldehyde temperature dependent reactivity on both the **(0001)** and **(10$\bar{1}$0)** surfaces is given in section 3.3.1. Sections 3.4.1.1 through 3.4.1.3 present the results from geometry optimized DFT calculations of H_2, CO, and CH_3O^- on the **(0001)** surface along with their binding energies. Similar calculations were performed for the surface bound formyl intermediate (section 3.4.2). The calculated results of attack by a proton on the formyl anion, both in the gas phase and on the surface, are presented in section 3.4.3. Section 3.4.4 probes the origin of the gas phase barrier to the *trans*-HCOH to CH_2O rearrangement. This calculation is extended to the ZnO surface in section 3.4.5. The MSR reaction coordinate is assembled from the previous sections and presented in section 3.4.6. The MSR reaction coordinate and the change in the reaction barrier are discussed in section 4.

2. Experimental Section

PES. The ZnO**(0001)** and ZnO**(10$\bar{1}$0)** surfaces used in this study were 1 mm × 1 mm plates cut from single crystals and oriented to 1° by Laue backscattering and then polished with successively smaller sizes of diamond grit until no surface pits were observed under a low power microscope (∼10×). They were then etched with HCl and rinsed thoroughly with deionized water. These surfaces were further cleaned in a vacuum by Ar^+ sputtering at successively 1000 V, and 500 V at 750 K, followed by annealing at this temperature. The cleanliness of these surfaces was checked by XPS spectroscopy.

Experiments using synchrotron radiation were performed at the Stanford Synchrotron Radiation Laboratory (SSRL) under dedicated operating conditions. For experiments in the VUV energy region a Grasshopper monochromator was used; a spherical grating monochromator was used for experiments in the soft X-ray region. A fixed photon energy resolution was maintained throughout these experiments: 0.2 eV for the Grasshopper and 0.5 eV for the spherical grating monochromators. A Perkin-Elmer Phi UHV system having a double pass cylindrical mirror energy analyzer (DPCMA), ion sputtering gun, and base pressure of 3×10^{-10} Torr was used for these experiments. For the studies performed on the Grasshopper monochromator the electron energy resolution of the DPCMA was maintained at 0.2 eV, and for the soft X-ray studies the DPCMA resolution was set at 0.5 eV. For all NEXAFS measurements wider slits were used (∼1.0 eV) to increase the instrumental signal-to-noise. The incident synchrotron radiation was maintained at 75° with respect to the DPCMA central axis, and thus impinged on the sample at close to a grazing angle. The photon flux was monitored by collecting the total electron yield from a high transmission grid in the UHV system. Clean background spectra were subtracted from the variable-energy valence band spectra of the surfaces with adspecies present by scaling the clean spectrum 3d band to the covered spectrum. The resulting difference spectrum was then fit with Gaussian/Lorentzian peaks by a curve-fitting procedure, which varies their position, width, and height while minimizing the difference between the fit and experimental spectra. All spectra have been referenced to the vacuum level due to the effects of sample charging at the low temperatures used in this study.[39]

The samples were heated and cooled in situ with the sample temperature measured by a thermocouple directly attached to the sample holder.

The CH_2O used in this study was produced from the thermal decomposition of paraformaldehyde (Aldrich) at approximately 390

(33) Jones, P. M.; May, J. A.; Solomon, E. I. *Inorg. Chim. Acta* **1998**, *275−276*, 327−333.
(34) Collman, J. P.; Hegedus, L. S. *Principles and Applications of Organotransition Metal Chemistry*; University Science Books: Mill Valley, CA, 1980.
(35) Stanton, R. V.; Merz, K. M. *J. Chem. Phys.* **1994**, *100*, 434.
(36) Deng, L.; Ziegler, T.; Fan, L. *J. Chem. Phys.* **1993**, *99*, 3823.
(37) Osamura, Y.; Goddard, J. D.; S., H. F., III. *J. Chem. Phys.* **1981**, *74*.
(38) Abashkin, Y.; Ruso, N.; Toscano, M. *Theor. Chim. Acta* **1995**, *91*, 179−186.
(39) Watson, R. E.; Perlman, M. L.; Davenport, J. *Surf. Sci.* **1982**, *115*, 117.

K.[40] The mass spectrum of the resulting CH_2O (UTI 100C) was free of methanol and methylformate. All gases were introduced into the experimental chamber via a separate Varian leak valve attached to an independently pumped, gas manifold. Gas exposures were monitored with a nude ionization gauge that was uncorrected for sensitivity.

Calculations. Electronic structure calculations were performed using density functional theory (DFT) as implemented in the Dmol computer code.[41,42] The BLYP (Becke, Lee, Yang, Perdew[43−45]) nonlocal density functional, or generalized gradient approximation (GGA) was used as it best describes weak bonding interactions.[46] Polarization functions were included in the numerically derived atomic basis sets, except where noted. This form of the basis set is known to yield accurate geometries and has been shown to be equivalent to Gaussian 6-31* basis sets.[41] The SCF calculations were considered converged when the largest deviation between cycles was less than 10^{-6} and was usually achieved in less than 100 cycles. To improve SCF convergence charge smearing was allowed for orbitals within 0.01 Ha of the Fermi level. All geometry optimizations utilized the Broyden−Fletcher−Goldfarb−Shanno (BFGS) Hessian update method.[47−50] The geometry was considered converged on the basis of the iterative change in bond length, energy, and force gradient (5.0×10^{-3} Å, 2×10^{-5} Ha, and 1×10^{-2} Ha/bohr, respectively). Convergence was usually attained in less than 200 iterations. Transition state searching employed the Hessian updating scheme of Powell using a normal mode following algorithm developed and implemented by Baker.[51] The lowest Hessian mode was chosen for this purpose. The transition state was considered converged on the basis of the iterative change in displacement, energy, and force gradient. These values were kept constant at 5.0×10^{-3} Å, 2×10^{-5} Ha, and 1×10^{-2} Ha/bohr, respectively (except where noted in the text). The transition state was usually located in less than 250 iterations. The atomic charges and the atomic character of the molecular orbitals were determined from Mulliken population analysis.[52]

The $Zn_{22}O_{22}$ cluster used in the DFT calculations is given in the Supporting Information. The geometry and composition of this cluster model closely follow Casarin et al. and are described in detail elsewhere.[31,32,53−55] The cluster is terminated with **(0001)** and **(000$\bar{1}$)** surfaces on opposite sides and is composed of four layers, which has been found to be sufficient to study surface adsorption at the central C_{3v} Zn^{2+} site on the **(0001)** surface. The Zn−O bond length was maintained at 1.978 Å, except where noted. This cluster model has been saturated with "pseudo atoms" to model the effects of an embedding scheme and thus the proper surface electronic environment. All of the coordinatively unsaturated oxygen atoms in the cluster, including the **(000$\bar{1}$)** surface, have been terminated with "pseudo atoms" (see Supporting Information) each with a valence charge of $0.5|e|$. The bond length of each O pseudo atom was set at 1.088 Å. The coordinatively unsaturated Zn atoms, except for those on the **(0001)** surface sites, were also saturated with pseudo atoms having a charge of $1.5|e|$ and a bond length of 1.625 Å, respectively. A charge of +5 was used for all calculations of cluster and neutral surface complexes. Casarin and co-workers have shown that by adjusting the atomic charges in this manner the calculated results, for a range of surface interactions, more closely reproduce the experimental data. Since heterolytic cleavage dominates on metal oxide surfaces, the total cluster charge was adjusted (positively or negatively) when ionic surface adsorbates were considered.

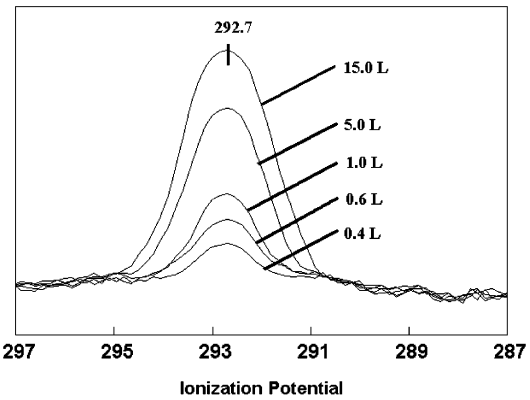

Figure 1. C1s XPS spectra of ZnO**(0001)** with increasing CH_2O exposure (0.4 L to 15.0 L) acquired at 130 K and $h\nu = 360$ eV.

3. Results and Analysis

3.1. Spectroscopy of CH_2O on ZnO. 3.1.1. XPS Studies of CH_2O on ZnO(0001). Figure 1 presents the C1s XPS spectra ($h\nu = 360$ eV) of the clean ZnO**(0001)** surface maintained at 130 K and exposed to increasing dosages of formaldehyde (0.4, 0.6, 1.0, 5.0, 15.0 L). A single symmetric peak at 292.7 ± 0.2 eV ionization potential (IP) is observed at low exposure (0.4 L) and grows in intensity with increasing formaldehyde exposure (15.0 L), which is assigned to the surface bound formaldehyde on the basis of its energy position and standard literature values.[56,57]

A surface chemisorption relaxation correction to the C1s energy of gas phase CH_2O can be estimated using the carbon K_{VV} Auger energy of the CH_2O surface species (262.0 ± 0.5 eV) and the shift, from gas phase, in its highest energy valence band PES peak[23,24] (-0.7 ± 0.1 eV, vide infra). This yields a formaldehyde C1s energy position of 291.9 ± 0.2 eV. Comparison of this corrected energy position to that of the chemisorbed CH_2O indicates the latter to be at approximately 0.8 eV higher energy.[58] This relaxation corrected result indicates that the chemisorbed formaldehyde is molecular but has a more positively charged carbon atom than gas phase formaldehyde.

3.1.2. NEXAFS of Low Coverage CH_2O on ZnO(0001). The carbon Auger yield NEXAFS spectrum of the molecularly chemisorbed CH_2O on the ZnO**(0001)** surface (130 K, 1.0 L) is shown in Figure 2. Two peaks are observed; the lowest energy feature is

(40) Abbas, N. M.; Madix, R. J. *Appl. Surf. Sci.* **1981**, *7*, 241.
(41) Delley, B. *J. Phys. Chem.* **1990**, *92*, 508−517.
(42) Delley, B. In *DMOL, a Standard Tool for Density Functional Calculations: Review and Advances*; Seminario, J. M., Politzer, P., Eds.; Elsevier Science B.V.: Amsterdam, 1995; Vol. 2, pp 221−254.
(43) Lee, C.; Yang, Y.; Parr, R. G. *Phys. Rev. B* **1988**, *37*, 785.
(44) Becke, A. D. *Phys. Rev. A* **1988**, *38*, 30989.
(45) Perdew, J. P.; Wang, Y. *Phys. Rev. B* **1992**, *45*, 13244.
(46) Fan, L.; Ziegler, T. *J. Am. Chem. Soc.* **1992**, *114*, 10890−10897.
(47) Broyden, C. G. *J. Inst. Math. Appl.* **1970**, *6*, 23.
(48) Fletcher, R. *Comput. J.* **1970**, *13*, 317.
(49) Goldfarb, D. *Math. Comput.* **1970**, *24*, 23.
(50) Shanno, D. F. *Math. Comput.* **1970**, *24*, 647.
(51) Baker, J.; Bergeron, D. *J. Comput. Chem.* **1993**, *14*.
(52) Mulliken, R. S. *J. Chem. Phys.* **1955**, *23*, 1883−1846.
(53) Casarin, M.; Maccato, C.; Tabacchi, G.; Vittadini, A. *Surf. Sci.* **1996**, *352−354*, 341−345.
(54) Casarin, M.; Favero, G.; Tondello, E.; Vittadini, A. *Surf. Sci.* **1994**, *317*, 422.
(55) Casarin, M.; Tondello, E.; Vittadini, A. *Surf. Sci.* **1994**, *307−309*, 1182.
(56) Au, C. T.; Hirsch, W.; Hirschwald, T. *Surf. Sci.* **1989**, *221*, 113.
(57) Yates, J. T.; Madey, T. E.; Erickson, N. E.; Worley, S. D. *Chem. Phys. Lett.* **1976**, *39*, 113.
(58) Seigbahn, K.; Nordling, C.; Johansson, G.; Hedman, J.; Heden, P. F.; Hamrin, K.; Gelius, U.; Bergmark, T.; Werne, L. O.; Manne, R.; Baer, Y. *ESCA Applied To Free Molecules*; North-Holland: Amsterdam-London, 1969.

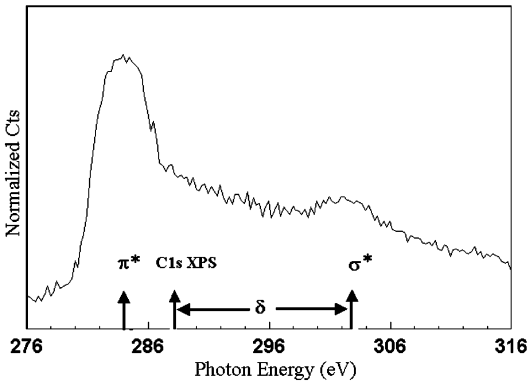

Figure 2. NEXAFS spectrum of CH_2O on ZnO**(0001)** acquired at 130 K and normalized to the incident photon flux. The covered spectrum was divided by a clean ZnO**(0001)** spectrum taken at the same temperature and instrumental resolution.

centered at 284.0 ± 0.2 eV and is ascribed to a π^* resonance.[59] The second, a broad peak centered at 302.6 ± 0.2 eV, is assigned to a σ^* shape resonance, which is due to the scattering of the outgoing photoelectron by the interatomic potentials.[60] Stohr et al.[61,62] have shown that the energy position of this resonance is sensitive to the C−O bond length.[59,63] They have derived a semiempirical expression that relates the energy separation, δ, between the C1s XPS position, referenced to the Fermi level (Figure 2), and the observed σ^* positions for a series of similar surface bound molecules. δ is found to be 14.6 eV for CH_2O bound to the ZnO**(0001)** surface. For comparison, δ for gas phase CH_2O is 14.6 eV.[64] Thus little or no change in the C−O bond length is observed upon chemisorption of the CH_2O to the ZnO surface (<0.05 Å). The accuracy of this comparison, between the experimental and the gas phase, is dominated by the assignment of the σ^* peak position and is determined by the accuracy of the monochromator (±0.2 eV) over the energy range of the transition. The intrinsic accuracy of this method (±0.05 Å) is sufficient to probe the expected large increases in the C−O bond length when CH_2O is bonded in an η^2 configuration in transition metal complexes (0.1 Å to 0.38 Å).[65−67] Thus the lack of C−O bond elongation and increased positive charge on carbon in the chemisorbed species are consistent with the CH_2O being bound to the ZnO**(0001)** surface in an η^1 configuration.

3.1.3. Variable Energy PES of CH_2O/ZnO(0001). Valence band PES spectra of the molecularly chemisorbed CH_2O on the ZnO**(0001)** were collected to elucidate the electronic structure of the surface complex. Figure 3A (top) are the PES spectra of both the clean ZnO**(0001)** (dashed curve) and the formaldehyde covered ZnO**(0001)** (solid curve) surfaces ($h\nu = 50$ eV) acquired at 130 K. The electronic structure of ZnO has been previously studied,[19,68−70] with the peak centered at 16 eV ionization potential assigned to the Zn 3d band and the asymmetric peak found between 10 and 14 eV ionization potential as due to the oxygen 2p band. Subtraction

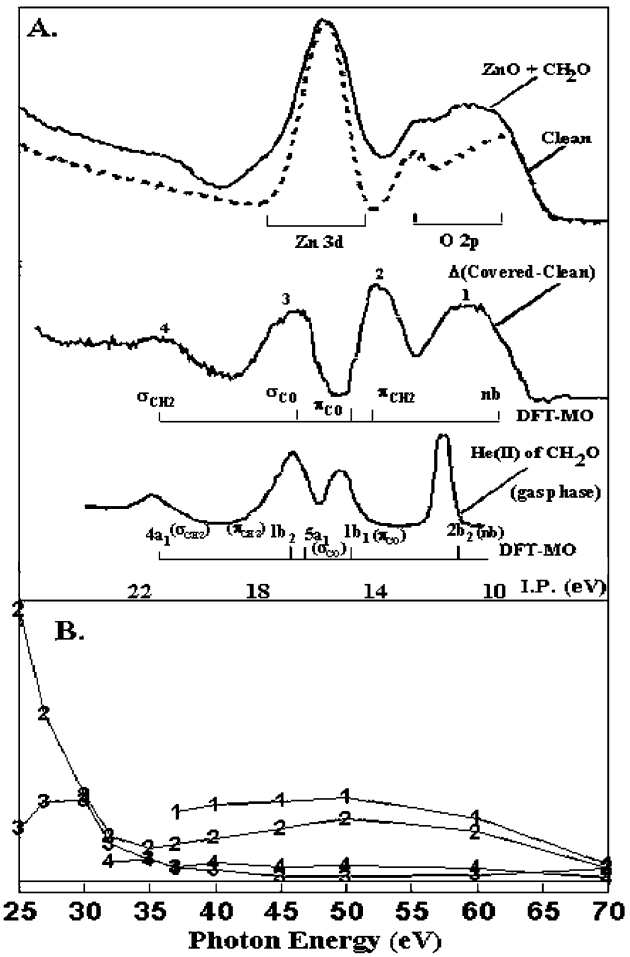

Figure 3. The photoemission spectra of CH_2O/ ZnO**(0001)** acquired at 130 K. (A) Upper panel: Clean ZnO**(0001)** spectrum (dashed line) with the CH_2O covered ZnO**(0001)** (solid line), acquired with $h\nu = 50$ eV. (A) Middle panel: The difference spectrum showing the formaldehyde peaks labeled 1 through 4 along with the DFT calculated formaldehyde and ZnO valence orbital positions. The gas phase spectrum and DFT calculations have been aligned at peak 4. (B) Photon energy dependence of the four formaldehyde induced peaks on ZnO**(0001)**.

of the clean ZnO**(0001)** from the CH_2O covered results in four CH_2O induced peaks (Figure 3A middle). The deepest energy peak at 21.2 eV IP, peak 4, is broad and rests on the rising secondary electron background. Peak 3 at 16.4 eV IP somewhat overlaps the high energy side of the Zn 3d. Peak 2 at 13.8 eV IP overlaps the low energy side of the Zn 3d, and the broad peak 1 is at 10.7 eV IP.

Variable energy photoelectron spectroscopy was used to probe the bonding interactions between the CH_2O levels and the Zn^{2+} site.[71] Figure 3B presents the variation in the integrated intensities of the four CH_2O peaks with incident photon energy. The intensity of peak 1 is masked by the large ZnO O2p signal at low photon energies so that no CH_2O signal is distinguished until 37 eV photon energy. Above this energy the peak 1 intensity is found to increase with photon energy with a broad maximum between 45 and 60 eV. This is consistent with Zn 3d character. Alternatively, if this peak were to have predominantly O2p character, an approximately

(59) Stohr, J.; Jaeger, R. *Phys. Rev. B* **1982**, *26*, 4111.
(60) Dehmer, J. L.; Dill, D. J. *J. Chem. Phys.* **1976**, *65*, 5327.
(61) Stohr, J., Hove, M. A. V., Tong, S. Y., Eds.; Springer-Verlag: Berlin, 1985.
(62) Stohr, J. *NEXAFS Spectroscopy*; Springer-Verlag: New York, 1992.
(63) Stohr, J.; Gland, J. L.; Eberhardt, W.; Outka, D.; Madix, R. J.; Sette, F.; Koestner, R. J.; Doebler, U. *Phys. Rev. Lett.* **1983**, *51*, 2414.
(64) Yukawa, Y. *Handbook of Organic Structural Analysis*; W. A. Benjamin, Inc.: Reading, MA.
(65) Huang, Y.-H.; Gladysz, J. A. *J. Chem. Educ.* **1988**, *65*, 298.
(66) Gambarotta, S.; Floriani, C.; C.-Villa, A.; Guastini, C. *J. Am. Chem. Soc.* **1985**, *107*, 2985.
(67) Buhro, W. E.; Patton, A. T.; Strouse, C. E.; Gladysz, J. A. *J. Am. Chem. Soc.* **1983**, *105*, 1056.
(68) Didzilius, S. V.; Cohen, S. L.; Butcher, K. D.; Solomon, E. I. *Inorg. Chem.* **1988**, *27*, 2238.
(69) Ivanov, I.; Pollman, J. *Phys. Rev. B* **1981**, *24*, 7275.
(70) Gopel, W.; Pollman, J.; Ivanov, I.; Reihl, B. *Phys. Rev. B* **1982**, *26*, 3144.
(71) Green, J. *Acc. Chem. Res.* **1994**, *27*, 131.

20-fold decrease in intensity would be expected (based on its cross section in this photon energy range). Since the Zn 3d cross section intensity is approximately 1 order of magnitude greater than the O2p and possesses a broad maximum in this photon energy range, the intensity in this peak (after subtraction) indicates that it contains a Zn 3d component that has been mixed into the CH_2O level. The observation of a delayed maximum results from the centrifugal barrier in the radial Schrodinger equation for an electron ionized from an orbital with $l = 2$.[72−76] Peak 2 displays high intensity at threshold and goes through a delayed maximum between approximately 50 and 60 eV. Peak 3 exhibits low intensity at threshold and rises to a maximum at approximately 30 eV, and thereafter decays to baseline. This cross sectional behavior is indicative of a shape resonance.[77,78] Prior gas phase studies of the photon energy dependence of the electronic energy levels of CH_2O have observed a similar shape resonance in the σCO energy level. In gas phase CH_2O this resonance was observed at approximately 25 eV photon energy. It has been noted that, upon bonding to the surface, resonances of this type shift toward higher energy by approximately 5 eV.[23] Peak 4 shows small intensity at threshold and no delayed maximum.

In order to facilitate the assignment of the CH_2O PES peaks on the ZnO**(0001)** surface the gas phase electronic structure of CH_2O is considered. Figure 3A (bottom) presents the He(II) UPS spectrum of gas phase CH_2O. This spectrum has been shifted to lower energy by 0.7 eV to align the deepest energy peak with the deepest energy peak in the CH_2O/ZnO**(0001)** subtracted spectrum. The calculated transitions from a full geometry optimized CH_2O DFT calculation (see section 3.2.1) are presented at the bottom Figure 3A. An excellent overall fit of the calculated formaldehyde energy levels (DFT-MO Figure 3A bottom) and the experimental gas phase data is observed. From these results the deepest energy peak at 21.2 eV IP in the gas phase spectrum is assigned to the $4a_1$ level, typically labeled σ_{CH2}. The next peak in the gas phase PES spectrum, at 16.2 eV IP, is due to the overlap of two levels. The higher energy of these, the $1b_2$, is principally a π-type interaction of the in-the-molecular-plane C2p and the H1s orbitals. It is referred to as the π_{CH2} molecular level. To lower energy is the $5a_1$, usually referred to as the σ_{CO}; this level is described by the DFT calculation as being dominantly composed of both C2s and $2p_z$ (z is along the C−O bond) orbitals. The next peak, $1b_1$, at 14.7 eV IP, is composed of an out-of-the-molecular-plane π bond between the carbon and oxygen atoms; this bond is polarized toward the carbon atom (section 3.2). This level is labeled the π_{CO}. The lowest energy peak, $2b_2$, at 11.2 eV is largely an oxygen lone pair and is considered a nonbonding level (nb).

Comparison of the CH_2O on ZnO**(0001)** subtracted spectrum to the gas phase CH_2O spectrum (Figure 3A middle to bottom) reveals a similar four peak pattern. However, the energy separations of individual peaks are different on the surface when compared to the gas phase. A comparison of peak 3 both in the gas phase and on the surface reveals little change in its energy position. The asymmetry in this peak is due to the subtraction process and its close proximity to the Zn 3d band. The variable energy PES data of peak 3 indicate the presence of a shape resonance in its cross section and unequivocally assign this peak as due to the σ_{CO}, $5a_1$ CH_2O level. Peak 2 undergoes an apparent 0.9 eV shift to lower energy when bound. We assign this peak to the near overlap of the $1b_2$ and $1b_1$ (π_{CH2} and π_{CO}, respectively) levels (vide infra). The π_{CH2} peak has undergone an approximate 2.8 eV destabilization due to its interaction with the ZnO surface. Peak 1, the $2b_2$, shifts to lower energy by 0.5 eV when bound, and this shift is due to its interaction with the Zn 3d at deeper binding energy.

Thus CH_2O is molecularly chemisorbed at low temperature and low coverage on the ZnO**(0001)** surface. Bonding does not significantly change the C−O bond length, consistent with an η^1 bonding geometry. CH_2O interacts with the Zn^{2+} site by donating charge and thereby increasing the net positive charge on the carbon atom thus shifting the C1s XPS peak position to deeper energy. Both formaldehyde $1b_2$ and $2b_2$ gas phase molecular orbitals shift to lower energy by 0.9 and 0.5 eV when CH_2O is bound to the ZnO surface.

3.2. Geometric and Electronic Structure of CH_2O on ZnO-(0001). 3.2.1. Geometry Optimized ZnO Cluster, CH_2O, and CH_2O/ZnO. As a prelude to studying the CH_2O/ZnO interaction, a geometry optimized DFT calculation was first performed using the $Zn_{22}O_{22}$ cluster (see Supporting Information) in which all except the central C_{3v} Zn^{2+} $(O^{2-})_3$ atoms were held constant (see Supporting Information). The optimized structure obtained has a calculated ionic charge of the nearest-neighbor **(0001)**-Zn ions to the Zn^{2+} C_{3v} surface site of $0.87|e|$, which is $0.37|e|$ less than the bulk Zn sites ($1.24|e|$).[52] This result is in reasonable agreement with prior studies using the same cluster model[31,32,53−55] and with recent solid state DFT-LCAO calculations indicating a significant charge transfer from the **(000$\bar{1}$)** to the **(0001)** surface, thereby lowering the ionicity of both surfaces.[79] There is a small 0.06 Å inward shift (from the **(0001)** surface toward the bulk) of the optimized surface Zn(II) site. This can be compared to the results of a recent surface X-ray diffraction study that reports a measured 0.14 Å inward shift of the Zn-**(0001)** sites.[79] This small change in the ZnO**(0001)** surface is due to the charge transfer to the 4s band of the Zn ions on this surface. Thus the ZnO cluster, with geometry optimization of the central C_{3v} site, is a reasonable model of the locally relaxed ZnO-**(0001)** surface.

Figure 4D presents the geometry optimized gas phase CH_2O species. The C−O bond length (1.217 Å), C−H bond length (1.114 Å), and H−C−O angle (122°) compare favorably to their experimental gas phase values, 1.206 Å, 1.117 Å, and 122° respectively.[64] The interaction of the CH_2O molecule with the ZnO**(0001)** surface was performed using the optimized ZnO cluster. This calculation was initiated by placing the formaldehyde above the central Zn^{2+} site and freezing all atoms except the formaldehyde and the central $Zn^{2+}(O^{2-})_3$ C_{3v} site. No restrictions were placed on the symmetry of the optimized binding site. In addition several different starting configurations were tested, including side-on (C−O bond parallel to the surface); however, all configurations optimized to the same final equilibrium geometry. Figure 5A presents the optimized ZnO-**(0001)**−CH_2O structure. CH_2O binds to this surface in an η^1 binding geometry with the oxygen end of the molecule closest to the Zn^{2+} site and having a slight misregistration of the central Zn^{2+} site and the oxygen of the formaldehyde (Figure 5A,C). The bound CH_2O molecule, with the ZnO cluster partially removed for clarity, is presented in Figure 5B,C. The calculated Zn−O bond is tilted away from the surface normal, giving a Zn−O−C angle of 123.3°. The

(72) Fano, U.; Cooper, J. W. *Rev. Mod. Phys.* **1968**, *40*, 441.
(73) Eastman, D. E.; Kuznietz, M. *J. Appl. Phys.* **1971**, *42*, 1396.
(74) Manson, T. M.; Cooper, J. W. *Phys. Rev.* **1968**, *165*, 126.
(75) Cooper, J. W. *Phys. Rev.* **1962**, *128*, 618.
(76) Yeh, J. J.; Lindau, I. *At. Data Nucl. Data Tables* **1985**, *32*, 1−155.
(77) Hermann, M. R.; Dierchsen, G. H. F.; Fatyga, B. W.; Langhoff, P. W. *Int. J. Quantum Chem., Quantum Chem. Symp.* **1984**, *18*, 719−734.
(78) Langhoff, P. W.; Orel, A.; Rescigno, T. N.; McKoy, B. V. *J. Chem. Phys.* **1978**, *69*, 4689.
(79) Wander, A.; Schedin, F.; Steadman, P.; Norris, A.; McGrath, R.; Turner, T. S.; Thornton, G.; Harrison, N. M. *Phys. Rev. Lett.* **2001**, *86*, 3811.

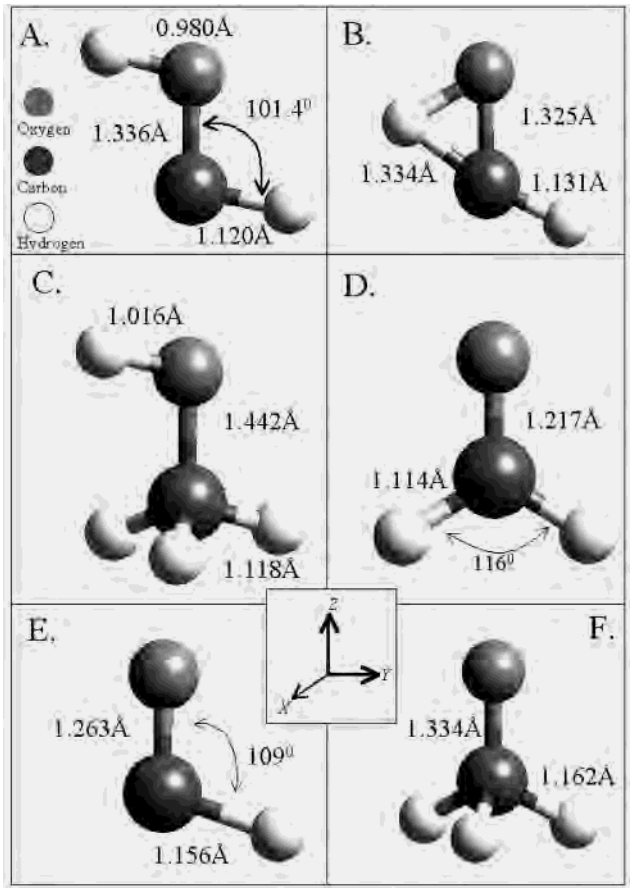

Figure 4. DFT geometry optimized gas phase structures of (A) *trans*-HCOH, (B) transition state between CH_2O and *trans*-HCOH, (C) CH_3OH, (D) CH_2O, (E) HCO^-, and (F) CH_3O^-.

tilt of the CH_2O takes place in the formaldehyde molecular plane, resulting in the optimized $Zn^{2+}-OCH_2$ unit in approximately the same plane (see Figure 5C) and reasonably aligned with a Zn−O bond. The $Zn-OCH_2$ bond length, 2.037 Å, is consistent with other similar η^1 bound aldehyde complexes, where the observed metal ion−oxygen distances range from 1.97 Å to 2.176 Å.[80−84] A small elongation of the C−O bond length to 1.225 Å, from its calculated gas phase value of 1.217 Å, is discernible. However, this result is at the limit of the resolution of the calculation (Δ bond length = 0.005 Å convergence). The NEXAFS data (see section 3.1.2), showing no or very little change in the C−O bond length, also supports a minimum change in this bond. In contrast, a significant change in the H−C−O bond angle (from the gas phase) is observed for the hydrogen closest to the surface (see Figure 5B). This angle has decreased from approximately 122° (gas phase) to 115°, bringing this hydrogen atom closer to the surface than at its gas phase value.

The energy due to the bonding of CH_2O to the ZnO**(0001)** surface, using the optimized structures, is calculated to be −15.2 kcal/mol. Heats of adsorption of approximately −15 kcal/mol have been experimentally observed for both η^2 and η^1 CH_2O on other metal oxide systems (Ru(001), oxidized Pd(111)2×2O and TiO_2-(001)).

Thus formaldehyde is calculated to be bound to the ZnO**(0001)** surface in an η^1 geometry, consistent with the C1s XPS results. The calculated C−O bond length of the surface bound CH_2O changes little from the gas phase, congruent with the NEXAFS result. In contrast, a significant change of the O−C−H angle is observed for the hydrogen atom closest to the surface.

3.2.2. Electronic Structures of CH_2O and CH_2O/ZnO. To ascertain changes in the electronic structure of formaldehyde due to bonding to the surface it is useful to first consider the molecular orbitals of gas phase CH_2O. These levels were described in section 3.1.3, and only the important levels will be considered here. Table 1 gives the results of a Mulliken population analysis of the gas phase CH_2O orbitals. Figure 6A presents the electron density contour of the $1b_2$ (π_{CH2}) molecular level. This level contains 44% total H1s character with 35% C2py and 21% O2py in a π-bonding interaction (in the molecular plane). The CH_2O $2b_2$ (nb) orbital, presented in Figure 6B, is found 10.4 eV above the $4a_1$. It may be thought of as the in-the-molecular-plane π^* interaction between the C2p and the O2p (Figure 7B). This level is highly polarized toward the oxygen (73% O2p character). It is typically described as an oxygen lone pair and is considered a nonbonding level (nb, with respect to the C−O bond).

The atomic components and energy position of the CH_2O-Zn^{2+} geometry optimized formaldehyde molecular orbitals are given in Table 2. The energy of the deepest level ($4a_1$) has been set to zero. Significantly, the energy order of these levels changes from their gas phase order. The level at 4.9 eV, the $5a_1$, is polarized toward the oxygen, lacks hydrogen content, and is assigned to the σ_{CO}. The σ_{CO} has a known shape resonance in its variable energy cross section, consistent with the PES data presented in Figure 3B.[78] The $1b_1$, at 6.6 eV, is highly polarized toward the oxygen atom. This level contains no hydrogen or metal ion character. Next, the $1b_2$ or π_{CH2} level is now between the $1b_1$ (out-of-plane π) and the nonbonding (oxygen lone pair) levels. Its energy position (7.4 eV) indicates that it is destabilized relative to the gas phase (by 2.8 eV). An examination of its atomic character (Table 2) reveals the presence of both 4% Zn 3d and 3% Zn 4s, 4p components. The presence of Zn 3d character is supported by the variable energy PES data for peak 2 (Figure 3B). Since the Zn 3d atomic cross section in this photon energy range is approximately 10 times greater than the O2p or C2p and the calculated orbital composition is dominated by these orbitals, a 3−4% Zn 3d content is expected to significantly contribute to this intensity. An electron density contour of this level is shown in Figure 6C. A perturbation of the π_{CH2} is observed when the CH_2O is bound to the ZnO surface (compare Figure 6A and Figure 6C). Table 2 indicates that new C2s, $2p_z$ and O2s, $2p_z$ character have been mixed into this molecular orbital, rotating the orbitals in the CHO fragment away from the hydrogen atom closest to the surface. This decreases the overlap between the H1s and the hybrid orbital and depletes the electron density associated with the hydrogen closest to the surface in this level (6% versus 26% H1s on the farthest hydrogen atom, Table 2). Thus the change in the O−C−H bond angle, of the bound CH_2O and its interaction with the Zn^{2+} reduces the overlap between the H1s and the π_{CH2} hybrid orbital.

Small amounts of Zn 3d and 4p character are mixed into the π_{CH2} level (Table 2). Since the Zn 3d is at deeper energy, the $1b_2$ (π_{CH2}) level undergoes an antibonding interaction that destabilizes this level. The effect of the small amount of 3d character is visible in its electron density contour as a small pinched region between

(80) Caldarelli, J. L.; Wagner, L. E.; White, P. S.; Templeton, J. L. *J. Am. Chem. Soc.* **1994**, *116*, 2878−2888.
(81) Bullock, R. M.; Ricci, J. S.; Szalda, D. J. *J. Am. Chem. Soc.* **1989**, *111*, 2741−2743.
(82) Bullock, R. M.; Rappoli, B. J.; Samsel, E. G.; Rheingold, A. L. *J. Chem. Soc., Chem. Commun.* **1989**, 261−263.
(83) Foxman, B. M.; Klemarczyk, P. T.; Liptrot, R. E. *J. Org. Chem.* **1980**, *187*, 253−265.
(84) Mendez, N. Q.; Seyler, J. W.; Arif, A. M.; Gladysz, J. A. *J. Am. Chem. Soc.* **1993**, *115*, 2323−2334.

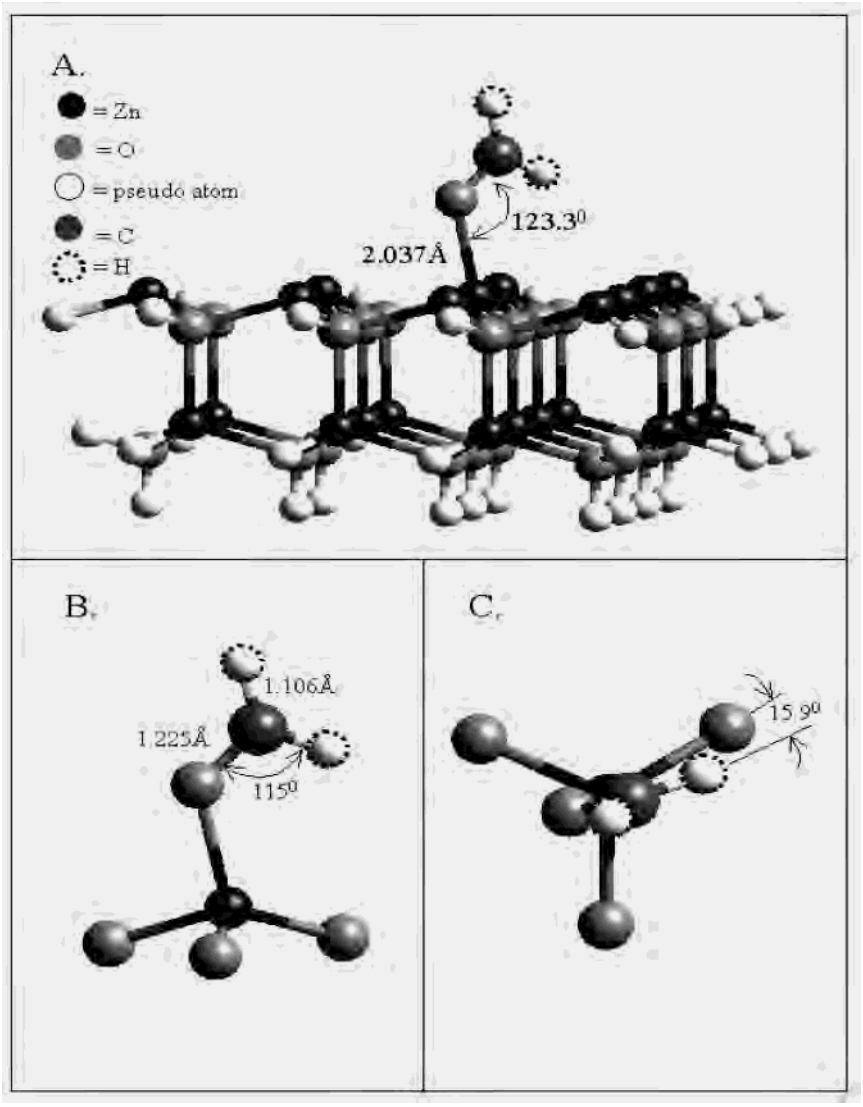

Figure 5. DFT geometry optimized structure of CH_2O/ZnO**(0001)**. (A) The entire ZnO cluster highlighting the CH_2O binding site. (B) CH_2O/ZnO**(0001)** binding site with the rest of the cluster removed for clarity. (C) CH_2O/ZnO**(0001)** binding site observed from above the surface plane, showing the dihedral angle between the Zn−O−H and the O^{2+}−Zn−O planes.

Table 1. DFT Calculated Gas Phase Energy Levels of CH_2O, Including Orbital Charge Decompositions

state	energy (eV)	C2s (%)	C2p_x (%)	C2p_y (%)	C2p_z (%)	O2s (%)	O2p_x (%)	O2p_y (%)	O2p_z (%)	H1s (%)
$2b_2$, nb	10.4	0	3	0	0	0	0	73	0	24
$1b_1$, π_{CO}	6.4	0	36	0	0	0	64	0	0	0
$5a_1$, σ_{CO}	5.3	8	0	0	13	15	0	0	56	8
$1b_2$, π_{CH2}	4.6	0	0	35	0	0	0	21	0	44
$4a_1$, σ_{CH2}	0	31	0	0	12	11	0	0	4	42

the Zn and oxygen atoms (see Figure 6C). Since both the Zn 3d and the π_{CH2} are filled, this interaction results in no net bonding. In contrast, the presence of Zn 4s, 4p character stabilizes the π_{CH2} orbital and results in net bonding between the Zn^{2+} and the CH_2O. Furthermore, this will remove electron density from the formaldehyde centered π_{CH2} molecular orbital and serve to lengthen the C−O bond.

The oxygen lone pair molecular orbital ($2b_2$ (nb), Table 2) contains both Zn 3d (6%) and Zn 4s, 4p (4%) content (see Figure 6D for contour) in agreement with the delayed maximum in the variable energy PES data for peak 1 (section 3.1.3). The presence of Zn 3d character in this molecular orbital destabilizes it from the gas phase by ∼1.3 eV. Its Zn 4p character implies a net bonding interaction with the Zn^{2+} metal ion. In contrast to the π_{CH2} level, a decrease of electron density in this π^* formaldehyde centered level should strengthen and therefore contract the C−O bond. However, this level is more accurately described as nonbonding with respect to the C−O bond and has less of an effect on the C−O bond length. Thus two formaldehyde levels contribute to the net CH_2O bonding to the ZnO: the $1b_2$ (π_{CH2}) and the nonbonding $2b_2$ (nb) molecular orbitals. The Zn 4s, 4p stabilizes both and has the net effect of little change in the bond length.

Formaldehyde is molecularly chemisorbed on the ZnO**(0001)** surface. This interaction takes place through the $1b_2$ (π_{CH2}) and $2b_2$ (nb) molecular orbitals donating into the Zn 4s, 4p levels forming a pseudo-σ bond. The Zn^{2+} is an acceptor; however, little change in the C−O bond is detected, indicating its stability toward further reaction. Both the bent Zn−O−C bond, ∼120°, and the contracted O−C−H angle (∼115°) place the closest hydrogen atom approximately 3.0 Å away from the surface and the carbon atom in proximity to the nearest neighboring Zn^{2+} (∼3.7 Å). This chemisorbed geometry can activate the CH_2O toward the possible transfer of an H^+ from the formaldehyde to the surface (section 3.3). This likely happens with the rearrangement of the formalde-

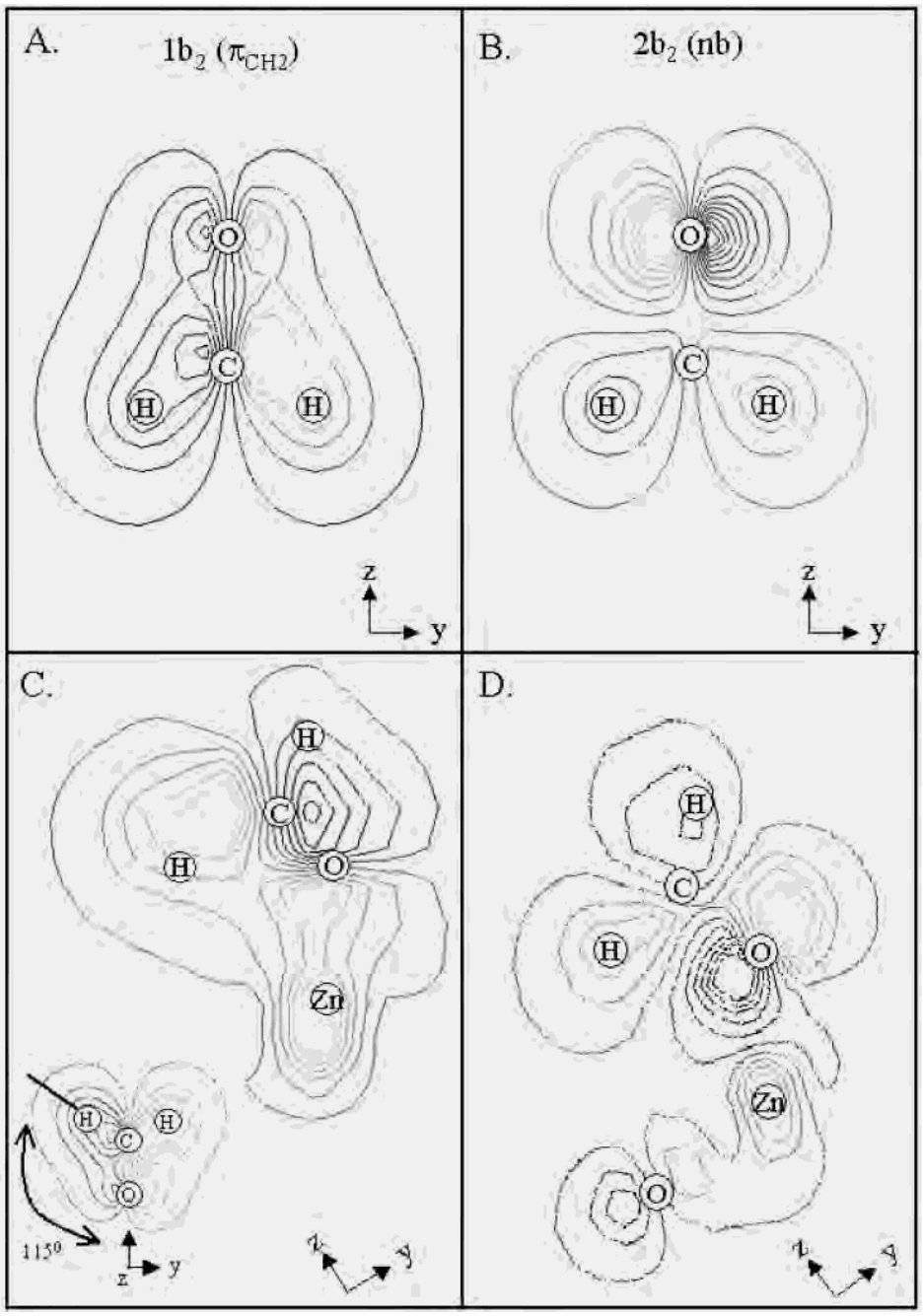

Figure 6. Density functional calculated orbital contours. Gas phase formaldehyde (A) π_{CH2} and (B) nb levels. Formaldehyde induced levels on the ZnO-**(0001)** cluster (C) π_{CH2} and (D) nb.

hyde on the surface (vide infra). The charge on the hydrogen closest to the Zn(II) is reduced from the gas phase and the farthest hydrogen atom ($-0.160|e|$, $-0.198|e|$, and $-0.189|e|$, respectively). This is a consequence of the lower overlap between the H1s and the remainder of the CH_2O π_{CH2} molecular orbital. This change is consistent with previous studies showing that the migrating hydrogen in the 1,2 hydrogen shift from CH_2O to HCOH acquires positive charge during its migration.[37]

3.3. Decomposition of CH_2O on ZnO. 3.3.1. Temperature Dependence of CH_2O on ZnO(0001) and ZnO($10\bar{1}0$). Chemisorbed CH_2O on the ZnO**(0001)** surface (15.0L) was stepwise heated from 130 K to 523 K. As shown in Figure 7A the C1s XPS data indicate a complex dependence on temperature. As the temperature of the chemisorbed CH_2O is raised from 140 K to 220 K, the central molecular CH_2O peak (292.7 eV) is attenuated and features are observed at higher and lower energies than this molecularly chemisorbed peak. This asymmetric broad peak was then peak fit revealing the overlap of the molecular peak (292.7 eV) with three additional peaks at 293.6 eV IP, 291.5 eV IP, and 290.2 eV IP (superimposed on the 220 K spectrum in Figure 7A). On the basis of our previous temperature dependent studies on the ZnO**(0001)** surface, the peaks at 293.6 eV and 290.2 eV are assigned to the surface bound formate[24,85] and methoxide,[24] respectively. The intermediate low energy peak at 291.5 eV is assigned in the next section to the surface bound formyl. After heating to the highest temperature (520 K) little molecular CH_2O remains bound to the surface and no methoxide or formyl is observed. The only significant peak remaining at 520 K is due to the surface bound

(85) Vohs, J. M.; Barteau, M. A. *Surf. Sci.* **1986**, *176*, 91.

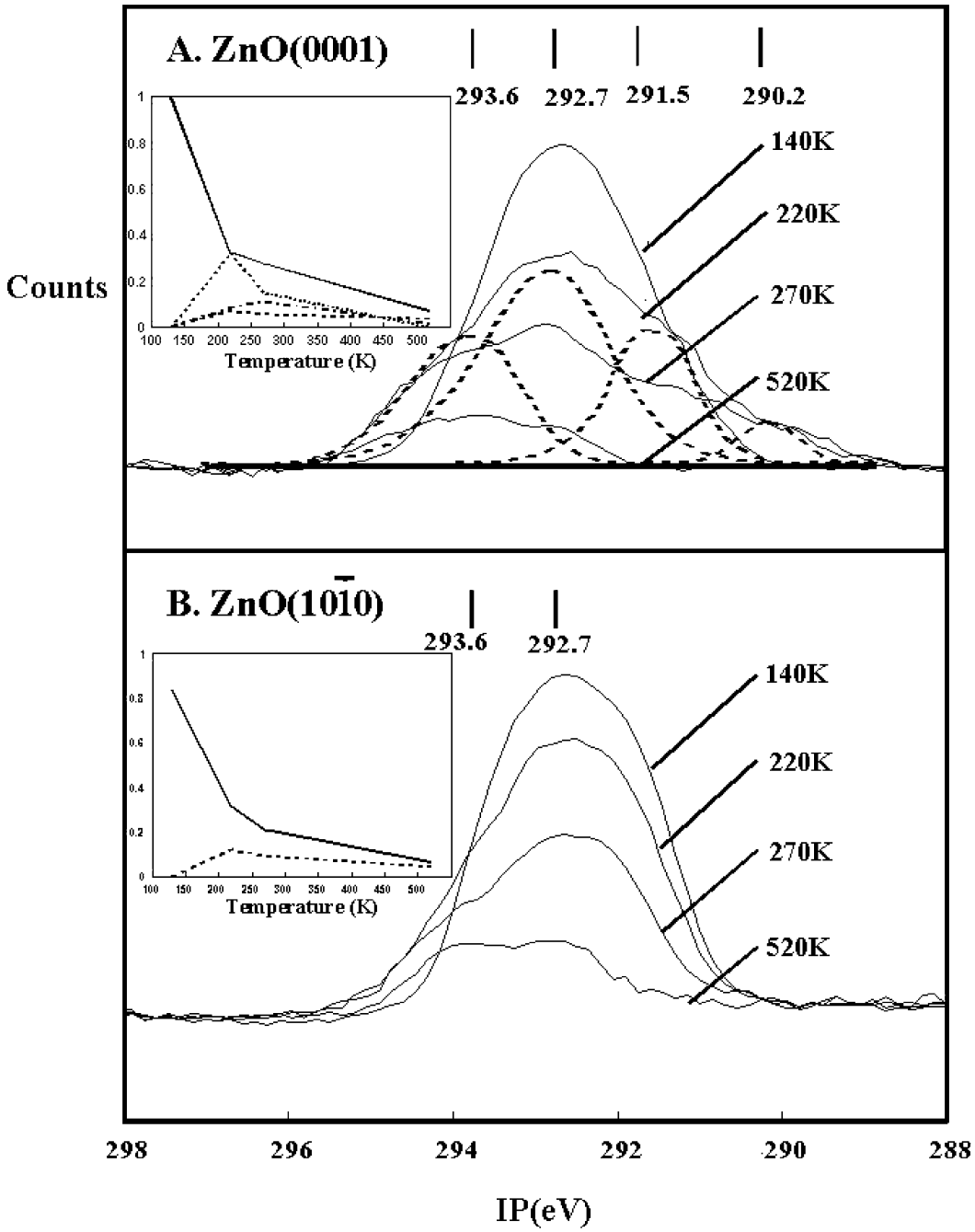

Figure 7. The C1s XPS spectra of stepwise heated chemisorbed formaldehyde on ZnO surfaces: (A) ZnO**(0001)** surface heated to 220 K, 270 K, and 523 K. The four peak fit to the 220 K spectrum is shown. (B) ZnO**(10$\bar{1}$0)** surface C1s XPS spectra of the heated (220 K, 270 K, 523 K) chemisorbed formaldehyde. Each spectrum was taken after a 60 s anneal at the temperature indicated and then cooled back to 130 K. All spectra were acquired using $h\nu = 360$ eV and normalized to the incident flux. Inset: Temperature dependence of the fitted peak areas (A) ZnO**(0001)** and (B) ZnO**(10$\bar{1}$0)** surfaces. The solid line is the fit to the molecularly chemisorbed peak, the dashed line to the formate peak, the dotted line to the methoxide, and the dash−dot line to the formyl surface species. All plotted areas were normalized to the observed 140 K molecular CH_2O peak.

Table 2. DFT Calculated Energy Levels of CH_2O/ZnO**(0001)**, Including Orbital Charge Decompositions

state	energy (eV)	C2s (%)	C2p$_x$ (%)	C2p$_y$ (%)	C2p$_z$ (%)	O2s (%)	O2p$_x$ (%)	O2p$_y$ (%)	O2p$_z$ (%)	Zn (%)	H (%)	H* (%)[a]
$2b_2$, nb	11.7	0	0	11	0	0	0	62	0	6% 3d, 4% 4p	14	9
$1b_1$, π_{CH2}	7.4	3	0	28	10	2	0	18	13	4% 3d, 2% 4p	26	6
$1b_2$, π_{CO}	6.6	0	34	0	0	0	66	0	0	0	0	0
$5a_1$, σ_{CO}	4.9	8	0	0	14	16	0	0	54	0	5	3
$4a_1$, σ_{CH2}	0	32	0	0	10	12	0	0	6	0	22	18

[a] H*, closest hydrogen atom to the Zn bonding site.

formate and a small amount of adventitiously readsorbed CH_2O. A profile of this temperature dependence is presented in the inset in Figure 7A. The individual peak intensity profiles have been normalized to the low temperature molecular CH_2O peak. The

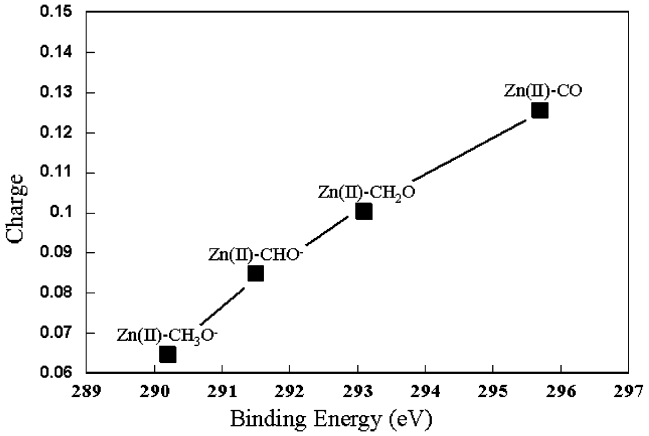

Figure 8. DFT calculated carbon charge in the geometry optimized CO, HCO^-, H_2CO, H_3CO^- surface species correlated with the relaxation corrected C1s XPS peak energies.

molecular chemisorbed formaldehyde peak drops in intensity as the temperature is raised to 220 K. Simultaneously the formate, formyl, and methoxide peaks appear. At this temperature both the formate and formyl peaks have similar intensities and the methoxide peak intensity is at a minimum. Both the formate and methoxide peaks increase in intensity with increased temperature. In contrast, the formyl intensity decreases with temperature. The simultaneous observation of methoxide, formate, and formyl at 220 K and the increase in intensity in both the methoxide and formate peaks, concomitant with a loss of intensity in the formyl peak, support its role as a possible intermediate in the formation of these species on this surface. At higher temperatures both the formyl and methoxide intensity decreases in a parallel manner and has little or no intensity at 523 K; however, the surface bound formate retains significant intensity at 523 K.

A similar experiment was performed on the ZnO**(10$\bar{1}$0)** surface. In contrast to the complex C1s XPS temperature dependence observed on the ZnO**(0001)** surface, increasing the temperature of formaldehyde on this surface reveals only the formation of the high energy formate peak (293.6 eV) throughout the temperature range probed (see Figure 7B). Further heating results in the attenuation of both the molecularly chemisorbed and the formate peaks. The integrated intensity of the individual peaks has been normalized to the low temperature molecular chemisorbed formaldehyde peak (Figure 7B, inset). The intensity of the CH_2O peak decreases with increasing temperature. Only 50% of the original peak remains on the surface at 220 K, and this fraction decreases to near zero at 523 K. In contrast, the formate peak intensity, after its formation ($\sim$220 K), rises to a small maximum at 273 K and thereafter slowly decays, reaching approximately 8% at 523 K. No other intermediates are observed on this surface at any temperature.

3.3.2. Assignment of the 291.5 eV Peak to Formyl. In the C1s energy region the observed chemical shift of a surface bound species is due to the charge of the atom under investigation and the screening effects due to the nearby surface.[23] Figure 8 presents a correlation of the calculated charge on the carbon atom of several observed and proposed intermediates on the ZnO surface and their experimental C1s XPS energy positions corrected for relaxation effects. CO, CH_2O, CH_3O^-, and the proposed CHO^- were bound to the central Zn(II) site on the previously described ZnO**(0001)** cluster model. Full geometry optimizations of the adsorbed species and the central ZnO_3 site were performed. The calculated carbon atom charge of each species was used in Figure 8. The C1s XPS positions of the CO and CH_3O^- species included in this figure have been previously reported,[23,24] CH_2O is reported in section 3.1, and the CHO^- intermediate is evaluated here. Figure 8 shows a clear increasing linear trend from the surface bound methoxide to the carbon monoxide. Both the carbon atom charge and the XPS peak energy position of the tentatively assigned formyl species are observed to be intermediate between the methoxide and formaldehyde. Chemical trapping techniques have been used to identify formyl in the gas stream above the ZnO based methanol synthesis catalyst under synthesis conditions,[86] and a ZnO bound formyl species has been observed, at 220 K, using FT-IR by Lavalley et al.[87,88] Bard et al. have detected surface formyl on a copper surface with C1s XPS;[89] its peak position was intermediate between methoxide and formaldehyde. Thus we assign the XPS peak at 291.5 eV resulting from the thermal decomposition of formaldehyde on ZnO**(0001)** to the formyl intermediate.

Formate is observed on both of the ZnO single crystal surfaces. In contrast, formyl and methoxide are observed only on the ZnO-**(0001)** surface, indicating that the observed decomposition is highly surface dependent. Previously it was shown that methanol is decomposed to methoxide over both the ZnO**(10$\bar{1}$0)** and **(0001)** surfaces;[24] however, no formate was formed from the decomposition of methanol over the ZnO**(10$\bar{1}$0)** surface. This effect was attributed to geometric differences between the surfaces. An important conclusion of that study indicated that formaldehyde was a necessary intermediate to form formate on the ZnO surfaces. The present decomposition study shows that CH_2O is stabilized on both ZnO surfaces and that its presence on the **(10$\bar{1}$0)** surface yields a surface bound formate. However, previous studies have shown that ZnO**(0001)** is the active surface for the methanol synthesis reaction.[29,30] Thus the concomitant formation of formate on the **(10$\bar{1}$0)** surface, in the same temperature range as the **(0001)** surface, indicates that this reaction path does not correlate with the known MSR ZnO surface activity on either surface. Therefore surface bound formate does not appear to be an important part of the methanol synthesis reaction over ZnO (starting from CO and H_2).

3.4. $CO + 2H_2 \rightarrow CH_3OH$ Reaction Coordinate. 3.4.1. Geometric and Electronic Structures of H_2, CO, and CH_3O^-/ZnO Surface Species. The methanol synthesis reaction taking CO to CH_3OH over a ZnO catalyst surface has been considered by Meutterties and Costa.[26,28] The double hydrogenation of carbon monoxide is thought to proceed through formyl, formaldehyde, and subsequently methoxide intermediates. Previous work from this laboratory and the present study provides spectra and structures of these proposed reaction intermediates. Below, we evaluate the energies of H_2, CO, and CH_3O^- binding on the ZnO**(0001)** surface using DFT with the ZnO cluster described above. We then examine formyl binding and its activation for reaction with a proton on the ZnO**(0001)** surface.

3.4.1.1. H_2/ZnO(0001). This calculation was performed by geometry optimizing the central $Zn(O)_3$ C_{3v} site of the cluster shown in the Supporting Information and an H_2 molecule with the side-on configuration above the Zn−O dimer. The optimized structure obtained is shown in Figure 9A (all atoms except the H_2 and central C_{3v} site have been removed). Hydrogen is calculated to dissociate over the model ZnO**(0001)** surface forming Zn−H and O−H. The calculated Zn−H and O−H bond lengths are 1.57 Å and 0.95 Å, respectively. The Zn−H bond is calculated to be perpendicular to

(86) Saussey, J.; Javalley, J. C.; Rais, T. *J. Mol. Catal.* **1984**, *26*, 159−163.
(87) Saussey, J.; Lavalley, J. C.; Lamotte, J.; Rais, T. *J. Chem. Soc., Chem. Commun.* **1982**, 278.
(88) Lavalley, J. C.; Saussey, J.; Rais, T. *J. Mol. Catal.* **1982**, *17*, 289.
(89) DeWulf, D. W.; Jin, T.; Bard, A. J. *J. Electrochem. Soc.* **1989**, *136*, 1686.

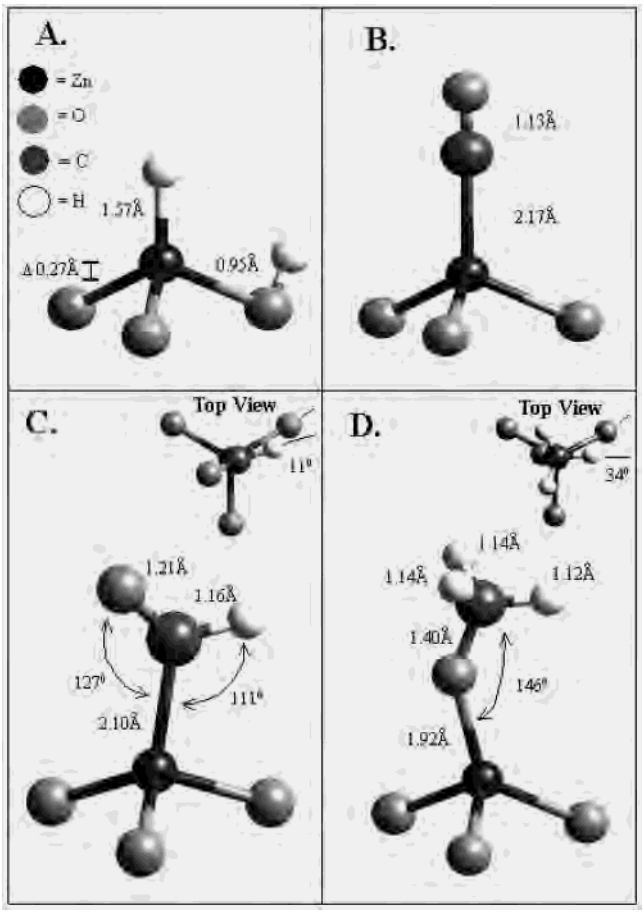

Figure 9. DFT calculated geometry optimized intermediates on the ZnO-**(0001)** cluster in the Supporting Information. (A) dissociated H_2, (B) CO, (C) HCO^- on ZnO**(0001)** including a top view (inset). (D) CH_3O^- including a top view (inset). For clarity only the surface intermediate and the $Zn(O)_3$ site are shown.

the surface plane, and the Zn−O−H angle is at approximately 90°, indicating that it is inclined away from the central Zn^{2+} site. The calculated Zn−H and O−H stretching frequencies, 1735 cm^{-1} and 3554 cm^{-1}, respectively, compare favorably with the experimental values, 1708 cm^{-1} and 3498 cm^{-1}.[90,91] Furthermore, a 0.27 Å outward shift in the Zn^{2+} is calculated upon binding H^-. Previous researchers have used ab initio methods to investigate the interaction of H_2 with both the **(0001)** and **(10$\bar{1}$0)** surfaces of ZnO. H_2 has been calculated to dissociate on the **(10$\bar{1}$0)** surface which "de-relaxes" both Zn and O atoms, displacing them outward from the clean surface.[92] The current study utilizes a nonlocal form of the exchange-correlation functional, which is known to correctly reproduce the bonding in weakly interacting systems,[46] and includes the optimization of the central C_{3v} site. The charge of the hydrogen bound to Zn^{2+} is calculated to be $-0.22|e|$ and only $+0.11|e|$ on the O^{2-} site. The calculated binding energy of H_2 with the Zn-**(0001)** surface is −15 kcal/mol, which compares favorably with the experimentally determined energy of −13 kcal/mol.[93]

3.4.1.2. CO/ZnO(0001). The interaction of CO with the ZnO surface has been extensively studied. This laboratory has probed the geometric and electronic structure of the CO/ZnO σ complex by applying XPS, UPS, variable energy PES, HREELS, and ARPES.[19,22,23,94−96] Casarin et al. have utilized local DFT theory and geometry optimization techniques to probe the CO/ZnO interaction theoretically.[31,32,97] In the present study nonlocal gradient corrected DFT, coupled with geometry optimization, is utilized. A geometry optimized gas phase CO molecule was placed above the central Zn^{2+} site of the ZnO cluster, and the central $Zn(O)_3$ site along with the CO was optimized. The final structure obtained is presented in Figure 9B (the central C_{3v}-CO site is shown). Carbon monoxide is calculated to bind to the Zn^{2+} site through the carbon atom in an η^1 geometry (Figure 9B). The calculated Zn^{2+}−C−O angle (180°) and Zn−C bond length (2.17 Å) are consistent with prior data and theoretical studies.[97] The C−O bond length is contracted (1.13 Å) from the optimized gas phase value of 1.136 Å (Figure 9B). NEXAFS data have shown that this bond length is contracted from its gas phase value by ∼0.03 Å.[23] Using the nonlocal density functional, a value of 2219 cm^{-1} is obtained for the frequency of the CO stretch, closely matching the experimental value of 2212 cm^{-1}.[98] The Zn^{2+}−CO bond is due to the charge transfer from the CO 5σ into the Zn4s and 4p_z levels; no π-back-bonding is observed. The present nonlocal DFT-MO results are consistent with this bonding description. A net $0.100|e|$ charge donation from the 5σ orbital into the Zn 4s, 4p orbitals is calculated. This donation, from the weakly antibonding 5σ molecular orbital, results in a small C−O bond length contraction. The calculated Zn^{2+}−CO bond energy is −9 kcal/mol, and the experimental value is −12 kcal/mol.[99]

3.4.1.3. CH_3O^-/ZnO(0001). The interaction of methoxide with the ZnO**(0001)** surface was previously studied using the Xα-SW formalism with the geometry fixed at values consistent with the inorganic literature.[24] In this study the geometry was optimized using GGA-DFT (BLYP) by placing the optimized methoxide anion (C−O bond length 1.334 Å and C−H = 1.162 Å) above the central C_{3v} site with the oxygen end facing the cluster. The optimized bound methoxide is presented in Figure 9D (methoxide and central Zn-$(O)_3$ site are shown). It is bound in an η^1 configuration through its oxygen. A small contraction in the C−O bond length is calculated for the surface bound methoxide compared to gas phase methanol (1.40 Å and 1.44 Å, respectively, see Figure 5C). This contraction is consistent with NEXAFS data.[24] The dihedral angle between the plane defined by the hydrogen atom closest to the O^{2-} and the C−O and the oxide−Zn−O plane is 34°, intermediate between the staggered and eclipsed conformations with the ZnO_3 C_{3v} site. The C−H bond length of the hydrogen atom closest to the oxide is approximately 0.02 Å shorter than the other two C−H bonds. The bound methoxide is misregistered with respect to the Zn^{2+} (Figure 9D inset). Previous Xα-scattered wave results using a fixed η^1 methoxide has assigned the surface bond to the overlap of the σ_O and σ_{CO} methoxide levels and the Zn 4s and 4p.[24] The present geometry optimized DFT-GGA results are consistent with this description. Furthermore the charges on the hydrogen atoms are negative, $\sim -0.051|e|$, with the charge on the hydrogen atom closest to the surface oxide, $\sim -0.064|e|$, consistent with our previous studies of this interaction.

(90) Ghiotti, G.; Chiorino, A.; Bocuzzi, F. *Surf. Sci.* **1993**, *228*, 287−288.
(91) Taylor, H. S.; Strother, C. O. *J. Am. Chem. Soc.* **1934**, *56*, 589.
(92) Zapol, P.; Jaffe, J. B.; Hess, A. C. *Surf. Sci.* **1999**, *422*, 1−7.
(93) Bolis, V.; Fubani, B.; Giamello, E.; Reller, A. *J. Chem. Soc., Faraday Trans. 1* **1989**, *95*, 855.
(94) D'Amico, K. L.; McClellen, M. R.; Sayers, M. J.; Gay, R. R.; McFeely, F. R.; Solomon, E. I. *J. Vac. Technol.* **1980**, *17*, 1080.
(95) Sayers, M. J.; McClellen, M. R.; Gay, R. R.; Solomon, E. I.; McFeely, F. R. *Chem. Phys. Lett.* **1980**, *75*, 575.
(96) McClellen, M. R.; Trenary, M.; Shinn, N. D.; Sayers, M. J.; D'Amico, K. L.; Solomon, E. I.; McFeely, F. R. *J. Chem. Phys.* **1981**, *74*, 4726.
(97) Casarin, M.; Maccato, C.; Vittadini, A. *Appl. Surf. Sci.* **1999**, *142*, 192−195.
(98) D'Amico, K. L.; McFeely, F. R.; Solomon, E. I. *J. Am. Chem. Soc.* **1983**, *105*, 6380.
(99) Solomon, E. I.; Jones, P. M.; May, J. A. *Chem. Rev.* **1993**, *93*, 2623.

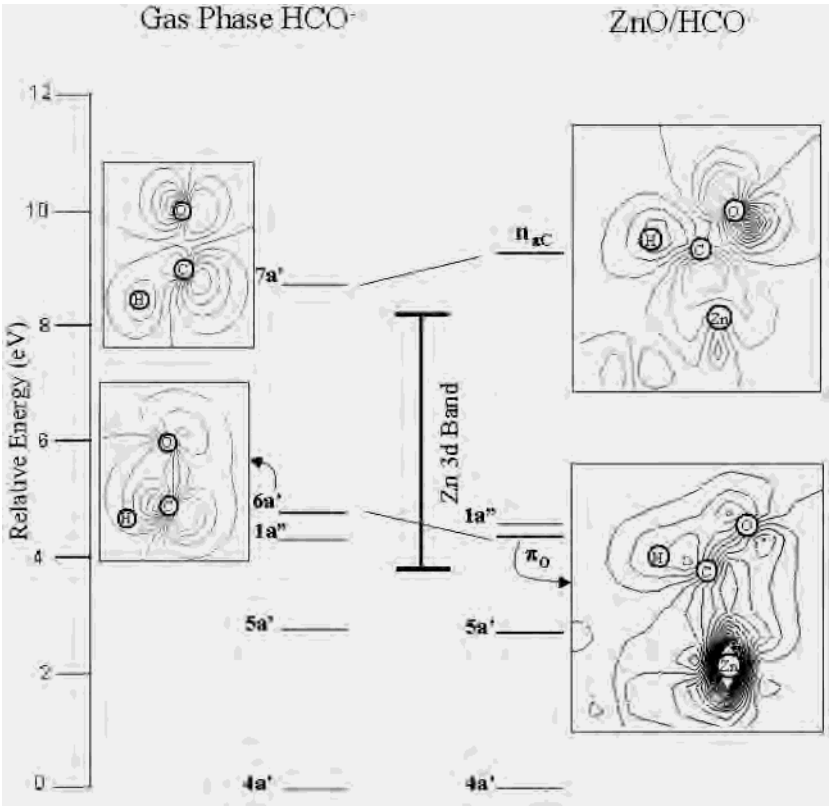

Figure 10. The energy level diagram for the gas phase (left) and ZnO**(0001)** bound HCO^- (right). Correlations of the gas phase 6a′ and 7a′ levels with the surface bound π_C and $n_{\pi C}$ states, respectively, are highlighted. The energy scale has been aligned at the deepest energy level. DFT orbital density diagrams for these states are included next to the energy level.

The methoxide surface bond energy, calculated from the optimized results, is −27 kcal/mol. Prior experimental and theoretical results suggest that the energy of this interaction is in the range −22 kcal/mol to −29 kcal/mol.[85,100]

3.4.2. Formyl Bonding to the ZnO(0001) Surface. Section 3.3 presented the thermal decomposition of formaldehyde on ZnO surfaces with the concomitant observation of formyl (at ∼220 K) on the **(0001)** surface. The optimized gas phase HCO^- structure is presented in the Supporting Information. The C−O bond in the gas phase formyl anion is calculated to be 1.263 Å, slightly longer than calculated for formaldehyde (1.217 Å). The H−C−O molecule is highly bent with an angle of 109°, and the H−C bond length is 1.156 Å.[101]

The calculated atomic components of the gas phase HCO^- molecular orbitals are also presented in the Supporting Information. Figure 10, left, presents the calculated energy level diagram along with pertinent contours of individual formyl molecular orbitals derived from the optimized structure. The energy of level 4a′ has been set to zero, and all others are referenced to this level. This level is due to the in-phase mixing of the hydride with the 4σ CO level, which also mixes with the 1π CO orbital. This is the principal interaction comprising the C−H bond. The 5a′ level is due to the in-phase mixing of the CO 5σ and the hydride. The second of the two degenerate CO π molecular levels (1a′) does not interact with the H, remains polarized toward the oxygen, and is best described as an oxygen lone pair. Level 6a′ is the out- of-phase combination of the hydride with the CO 1π. This level has ∼54% $O2p_y$ with little hydrogen content (Supporting Information), and may also be considered an oxygen lone pair. The HOMO level, 7a′, results from the in-phase interaction of the hydride and the CO 2π*, which is formally filled for this singly charged species. This level has a significant amount of electron density in an sp^2 hybrid and may be thought of as a carbon lone pair. However, it is important to note that the decomposition of this molecular orbital into atomic components also reveals 30% $O2p_y$ character (see Supporting Information).

The optimized gas phase HCO^- anion was placed above the cluster surface with the C−O bond parallel to the surface. The entire $Zn(O)_3$−HCO^- was then optimized. The resulting structure is shown in Figure 9C (central C_{3v} site and HCO^- are shown). The HCO^- is calculated to bond to the Zn^{2+} site in an η^1 geometry, through the carbon atom. The optimized C−O bond (1.21 Å), which is contracted from the calculated gas phase value ($\Delta \sim -0.05$ Å), and the Zn^{2+}−C bond (2.10 Å) are within the range observed in metal formyl complexes.[102] The Zn^{2+}−C−O angle is 127°, and the O−C−H angle has changed to 122° from 109° (gas phase), due to bonding to the surface.

The energy level diagram with pertinent density contours of the surface bound HCO^- is presented at the right of Figure 10. The atomic character of the formyl orbitals on the ZnO surface is presented in the Supporting Information. Only two levels change their energy position upon binding to the surface, the 6a′ and 7a′ orbitals. The 7a′ (labeled $n_{\pi C}$ in Figure 10) becomes destabilized by its interaction with the Zn^{2+} by approximately 0.7 eV. This level has 6% Zn 3d character. Since both the 7a′ and Zn 3d levels are filled, no net bonding can result from this interaction. The electron density contour of this level (in the Zn−HCO plane) clearly

(100) Bowker, M.; Houghton, H.; Waugh, K. C. *J. Chem. Soc., Faraday Trans. 1* **1981**, *77*, 3023−3036.
(101) Murray, K. K.; Miller, T. M.; Leopold, D. G.; Lineberger, W. C. *J. Chem. Phys.* **1986**, *84*.
(102) Wong, W. K.; Wilson, T.; Strouse, C. E.; Gladysz, J. A. *J. Chem. Soc., Chem. Commun.* **1979**, 530.

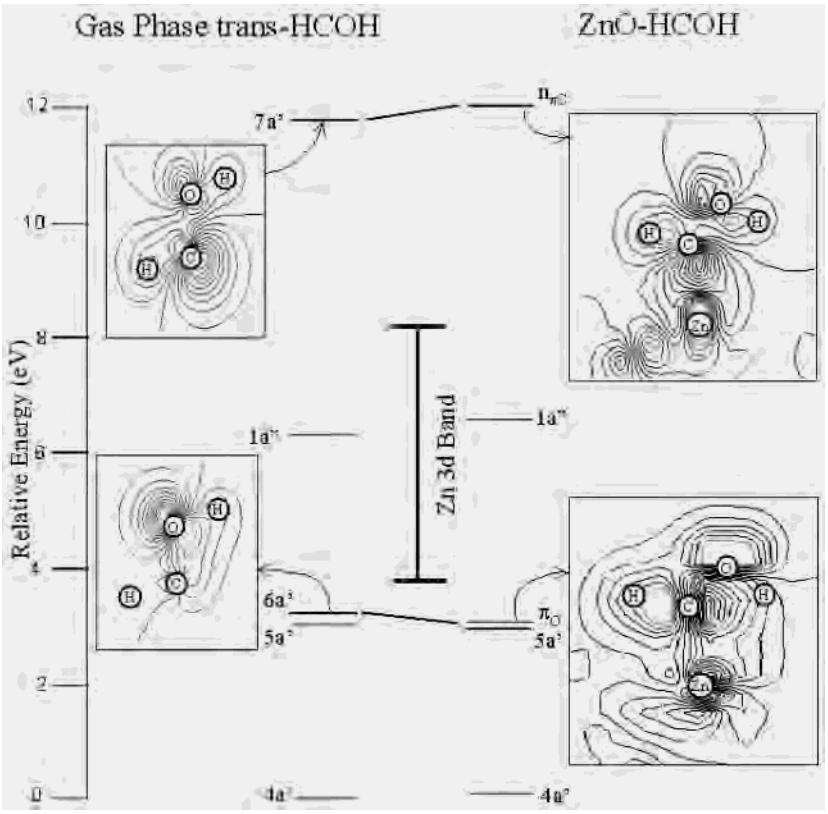

Figure 11. The energy level diagram of the gas phase *trans*-HCOH (left side) and the *trans*-HCOH bound to the ZnO**(0001)** surface (right side). The 6a′ and 7a′ levels of the optimized gas phase *trans*-HCOH correlated with the bound π_O and $n_{\pi C}$ states, respectively. The energy scale has been aligned at the deepest level. The DFT orbital contours are shown next to the associated levels.

indicates the presence of antibonding Zn 3d content (Figure 10, right side top inset). In addition to Zn 3d character, 2% Zn 4s, 4p character is also mixed into this level. This interaction results in net bonding between the HCO^- and Zn^{2+}. This level is antibonding with respect to the C−O bond so some bond strengthening would be expected due to donation to the Zn. This level ($n_{\pi C}$) has π lone pair carbon character. Next the HCO^- 6a′ molecular orbital has been stabilized by ∼0.5 eV, by its interaction with the Zn^{2+} (π_O). This stabilization is due to the mixture of Zn 3d and 4s, 4p (4% and 1%, respectively) character into this molecular orbital. Therefore, the bonding of the HCO^- to the ZnO surface involves two orbitals, the $n_{\pi C}$ and the π_O, which interact with the Zn 4s and 4p levels donating charge to the Zn^{2+}. As a result of its interaction with the Zn^{2+} site, the formyl anion is perturbed, and the carbon hybridization becomes more sp^2-like, yielding a significantly increased H−C−O bond angle to ∼122° and a contraction of the C−O bond (Figure 9C). The O character shifts from ∼30% (gas phase) to 49% ($n_{\pi C}$), and the atomic charge on the oxygen atom of the bound formyl anion is $-0.500|e|$. From frontier molecular orbital (FMO) theory *both the large occupied valence orbital coefficients and the sizable negative charge on the oxygen activate this atomic center for attack by a proton.*[103] The bonding energy of the HCO^- to the ZnO is −15 kcal/mol.

3.4.3. Geometric and Electronic Structure of Gas Phase and ZnO Bound *trans*-HCOH. The gas phase reaction of H^+ with HCO^- has been investigated to elucidate the most stable species obtained from attack at the oxygen and its interaction with the ZnO surface. This gas phase reaction is initiated by placing the H^+ in proximity to the O^- end of the HCO^- and optimizing the entire ensemble. Of the two conformers obtained, *cis*-HCOH and *trans*-HCOH, the trans species is the more stable by -4.9 kcal/mol, in agreement with earlier theoretical results.[35,36] The optimized gas phase *trans*-HCOH molecule is given in the Supporting Information. An elongation of the C−O bond is calculated (from 1.263 Å in HCO^- to 1.336 Å in *trans*-HCOH) which is consistent with loss of most of the double bond character in the C−O bond.[104] The calculated O−C−H bond angle, 101.4°, is considerably smaller than that found in the formaldehyde molecule, and the H−O−C angle is somewhat larger than observed in methanol (107.6° and 106.1°, respectively). These observations can be justified on the basis of the presence of resonance structure A in Scheme 1, with a single, elongated C−O bond (compared to formyl). In addition, the lone pair on the carbon in resonance structure A sterically repels the hydrogen, decreasing the H−C−O bond angle, relative to resonance structure B.

Scheme 1

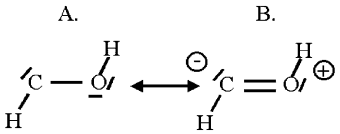

These results are consistent with previous theoretical studies of the 1,2 migration of hydrogen rearrangement of formaldehyde to *trans*-HCOH.[35] The energies and atomic components of the gas phase *trans*-HCOH molecular orbitals are collected in the Supporting Information. The gas phase energy level diagram is presented in Figure 11, left, along with the electronic density

(103) Fleming, I. *Frontier Orbitals and Organic Chemical Reactions*; John Wiley & Sons: New York, 1985.

(104) Pope, S. A.; Hillier, I. H.; Guest, M. F.; Colburn, E. A.; Kendrick, J. *Surf. Sci.* **1984**, *139*, 299−315.

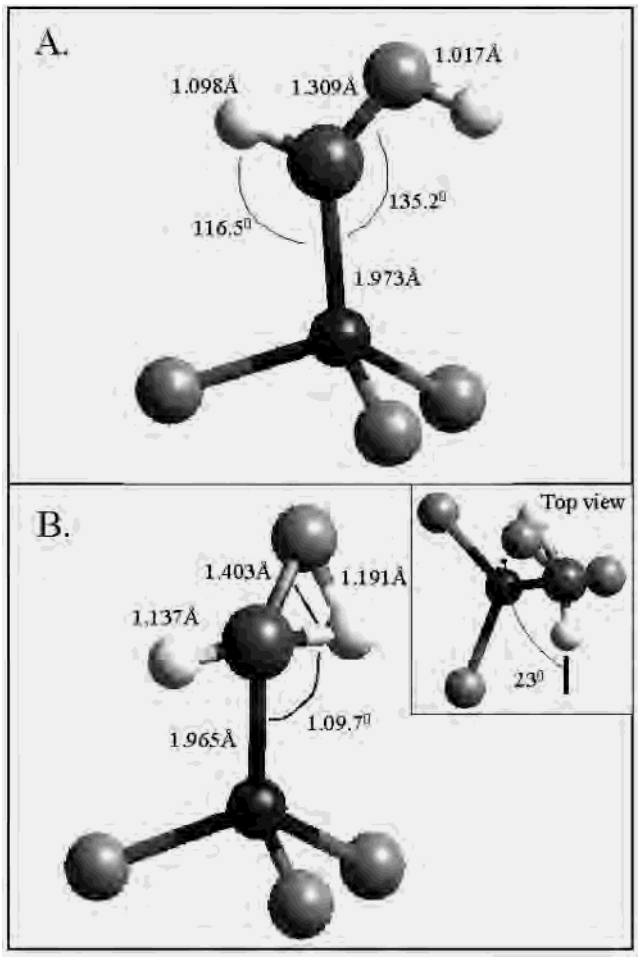

Figure 12. (A) The DFT geometry optimized planar *trans*-HCOH on the ZnO**(0001)** surface (model in Supporting Information). (B) Geometry of the transition state on the ZnO**(0001)** surface. The surface bound transition state has been shifted parallel to the surface and has a dihedral angle of ~23° (inset). The ZnO_3 binding site and bound species are shown for clarity.

contours of pertinent levels. The energy of the deepest level, 4a′, has been set to zero. The 4a′ is principally due to the overlap of the C2s and O2p_z with the H1s bound to the oxygen and dominates the O−H bond. Level 5a′ at ~3.0 eV is predominately an oxygen lone pair; however, it contains ~7% C2p_y character which contributes to an in-plane π interaction with the oxygen (see Supporting Information). The next level, 6a′, is the dominant C−H bonding interaction; it contains 38% H1s character. Level 1a″ is the out-of plane π bond. It is largely unaffected by the newly formed O−H bond. Finally, the HOMO level 7a′ has most of its electron density in a C2$p_{y,z}$ hybrid and may be considered a carbon lone pair. The electronic structure of the gas phase *trans*-HCOH exhibits only limited differences from the HCO^- gas phase determined structure.

The optimized gas phase *trans*-HCOH was placed above the $Zn_{22}O_{22}$**(0001)** model surface with the C−O bond aligned parallel to the surface and the carbon atom nearest the central Zn^{2+} site. The entire $Zn(O)_3$−HCOH was optimized. Figure 12A presents the fully optimized structure (C_{3v} site and the bound HCOH are presented). HCOH is calculated to bind to the Zn^{2+} site through the carbon atom in an η^1 geometry. The trans configuration is maintained upon binding, and the bound HCOH molecule is planar (Figure 12A). The Zn−C is 1.973 Å, and the Zn−C−O angle is 135.2°. The C−O bond, 1.309 Å, has contracted relative to the gas phase upon bonding to the surface. The C−H 1.098 Å and O−H 1.017 Å bonds have been contracted and lengthened respectively compared to the gas phase (Supporting Information), while the C−O−H bond angle decreases to ~101° from the gas phase value of ~106°.

Table 3. DFT Calculated Formyl Anion Energy Levels on ZnO**(0001)**, Including Orbital Charge Decompositions

state	energy (eV)	% C	% O	H1s	% Zn
$n_{\pi C}$	9.4	31	49	13	6% 3d, 2% 4s, 4p
1a″	4.4	33	64	0	0
π_O	4.2	30	49	4	4% 3d, 1% 4s, 4p
5a′	2.7	18	64	12	0
4a	0	36	24	37	0

Table 4. DFT Calculated *trans*-HCOH Centered Energy Levels on ZnO**(0001)**, Including Orbital Charge Decompositions

state	energy (eV)	% C	% O	% H 1s	% H* 1s	% Zn 4s, 4p
$n_{\pi C}$	12.1	47	12	2	7	5% 3d, 5% 4p
1a″	6.3	14	68	0	0	0
π_O	3.1	27	16	29	5	4% 3d
5a′	2.7	13	24	4	4	0
4a′	0	24	36	13	9	0

The electronic energy level diagram of the bound *trans*-HCOH is included on the right side of Figure 11. The lowest energy state has been aligned to the gas phase diagram on the left. Bonding to the ZnO perturbs two HCOH centered orbitals. This situation is similar to that encountered for the bound HCO^-. Pertinent electron density contours of these levels are included on the right of Figure 11. Table 4 presents the atomic composition of the orbitals of the bound HCOH. The levels labeled π_O and $n_{\pi C}$ are calculated to be ~0.3 V and ~0.5 eV stabilized and destabilized respectively relative to the gas phase. Each has Zn metal ion character. The level labeled π_O has 4% Zn 3d character, which stabilizes this level, and the $n_{\pi C}$ level has 5% Zn 3d and 4% Zn 4s, 4p, which both destabilizes and stabilizes this level, respectively. The effect of the Zn based atomic orbitals may be seen in the electron density contours as an antibonding region between the Zn and C centers in the $n_{\pi C}$ state, and a bonding region in the π_O. The presence of Zn 4s, 4p character in the $n_{\pi C}$ indicates that this level undergoes a net bonding interaction with the Zn^{2+}. Thus *trans*-HCOH binds to the ZnO-**(0001)** surface through a σ-type interaction with the HCOH $n_{\pi C}$. Since this level is antibonding with respect to the C−O bond, a net contraction in the C−O bond is observed in the bound HCOH species (Figure 12A). Furthermore, this level contains approximately 7% H1s character of the hydrogen bound to the oxygen atom. This bonding interaction leads to an elongation of the O−H bond. Last, the bound O−C−H angle increases from ~104° in the gas phase to ~108°, becoming more alcohol-like (Supporting Information). The energy of the *trans*-HCOH interaction with the ZnO surface is −19 kcal/mol.

3.4.4. Rearrangement of *trans*-HCOH to CH_2O. An important step in the sequential hydrogenation of CO to H_3COH proceeds through formaldehyde. As the formation of CH_2O (from H_2 + CO) is thermodynamically uphill, its interaction with the surface must substantially stabilize its formation.[105] Previous sections have presented both experimental and theoretical investigations of the interaction of CH_2O with the ZnO**(0001)** surface. This interaction was determined to take place through the oxygen atom of the formaldehyde. Thus starting from the carbon end bound CO and passing through the oxygen end bound formaldehyde, a surface rearrangement takes place that brings the oxygen atom of the

(105) Henrici-Olive, G.; Olive, S. *Catalyzed Hydrogenation of Carbon Monoxide*; Springer-Verlag: Berlin, 1984.

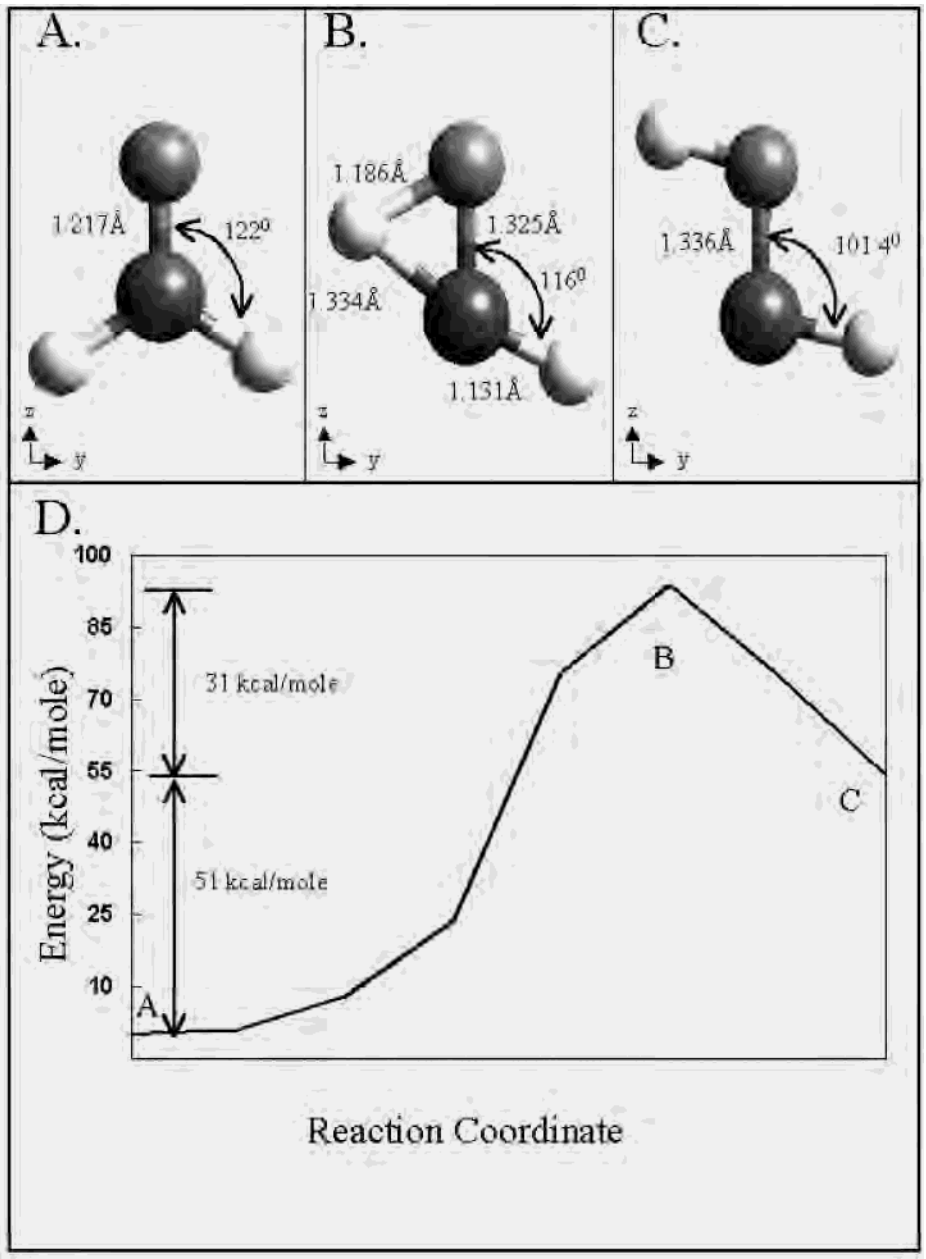

Figure 13. Reaction coordinate from *trans*-HCOH to H_2CO. (A) DFT geometry optimized gas phase formaldehyde. (B) Gas phase transition state observed at point B in the reaction coordinate shown in part D of this figure. The transition state is planar and has an elongated C−O compared to the gas phase CH_2O. (C) Optimized gas phase *trans*-HCOH. (D) Calculated energy profile along the hydrogen atom migration from CH_2O to *trans*-HCOH.

interacting species to the surface. From FMO theory the initial reaction of an H^+ with CHO^- yields a surface bound *trans*-HCOH (see section 3.4.3).[106] The gas phase rearrangement of the *trans*-HCOH, yielding formaldehyde, is known to take place with a substantial barrier. To illuminate how the rearrangement of HCOH to CH_2O is altered by bonding to the ZnO surface, we have undertaken a DFT-GGA calculation that identifies the transition state between these two stable conformers and the electronic structure contributions to this large rearrangement barrier.[107] The gas phase DFT transition state calculation was initiated from the *trans*-HCOH geometry, and a linear transit, transition state search calculation was performed (Figure 13D). Figure 13B presents the calculated transition state geometry along with the *trans*-HCOH (Figure 13C) and CH_2O (Figure 13A) for comparison. A vibrational calculation was performed using the obtained transition state geometry. One imaginary frequency was found. At the transition state the migrating hydrogen is approximately halfway between the carbon and oxygen atoms (Figure 13B). In this geometry the C−O bond has lengthened to 1.325 Å from the CH_2O gas phase (1.217 Å), and the C−H bond is now 1.131 Å. The O−C−H angle, 116°, is intermediate between that in the formaldehyde and the *trans*-HCOH, and the migrating hydrogen is 1.186 Å away from the oxygen atom. The transition state is calculated to be planar, in agreement with previous studies.[38] The reaction coordinate of the rearrangement is presented in Figure 13D. The calculated barrier at the transition state is ∼82 kcal/mol, and the energy difference between the *trans*-HCOH and formaldehyde is 51 kcal/mol; both are consistent with prior theoretical investigations.[35,36,38]

The electronic structure of the gas phase transition state is presented in Figure 14, left. The atomic composition of each

(106) Klopman, G. *J. Am. Chem. Soc.* **1968**, *90*, 223.
(107) Pancir, J. *Collect. Czech. Chem. Commun.* **1977**, *42*, 16.

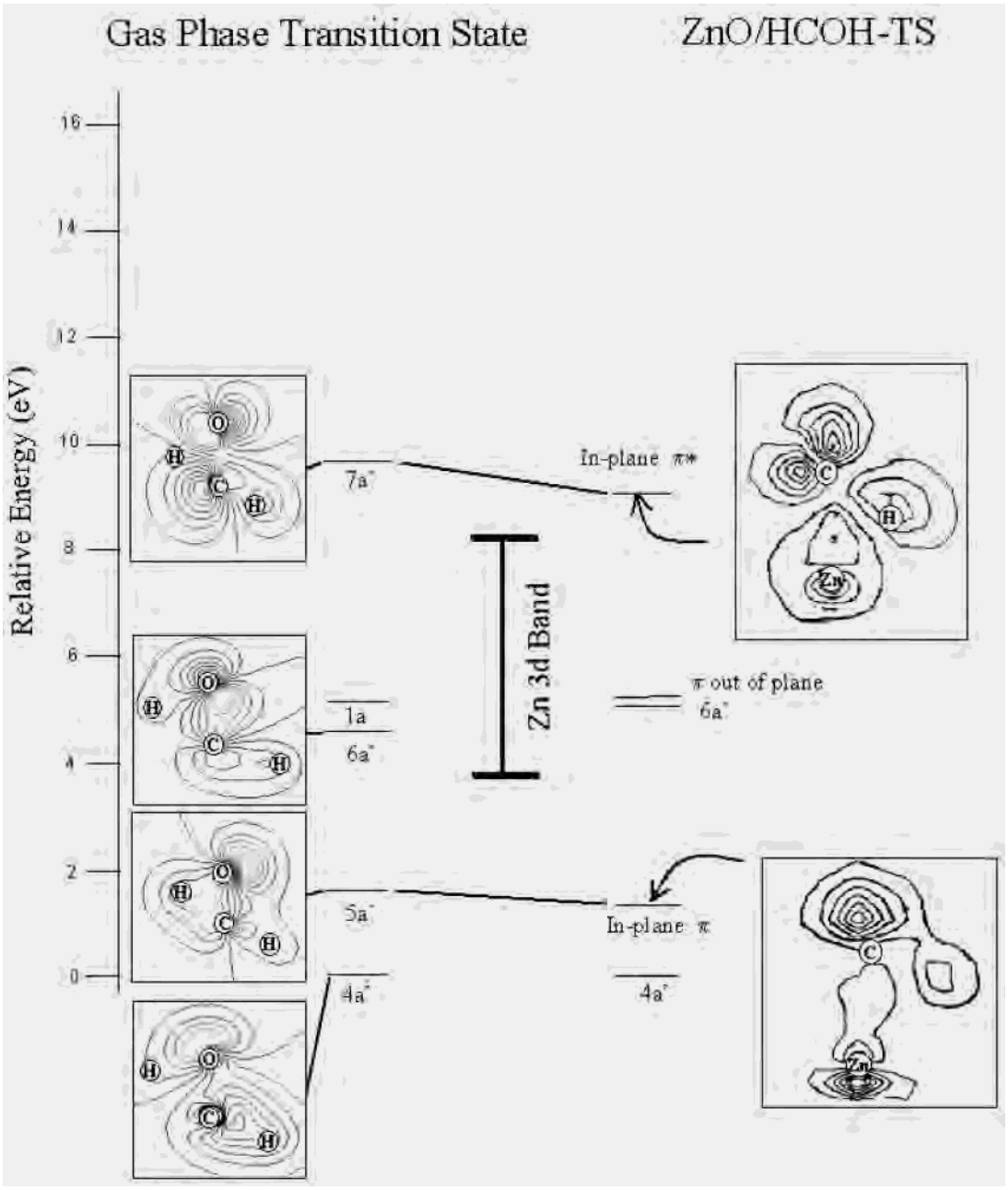

Figure 14. Energy levels of the (A) gas phase transition state and (B) ZnO**(0001)** bound transition state aligned to the deepest level. HCOH correlation of the gas phase 7a′ and 5a′ with the bound in-plane π^* and π levels, respectively. DFT electron density contours are shown with the associated energy level. Electron contour of the gas phase 6a′ state is included to highlight its bond to the migrating hydrogen atom.

molecular orbital is presented in the Supporting Information. Level 4a′ is a σ-type interaction between the carbon atom and its strongly bound hydrogen atom. It is similar to the previously described formaldehyde level labeled 4a′ (σ_{CH2} in Table 1). This level is perturbed by the absence of the migrating hydrogen atom. The next deepest level, 5a′, derives from the in-plane π-interaction between the carbon and the oxygen $2p_y$. With the migration of the hydrogen atom this level now contains significant $O2p_z$ character (14%, see Supporting Information) when compared to the *trans*-HCOH. The presence of this additional character rotates this molecular orbital toward the migrating hydrogen atom (Figure 14, left, 5a′). This level has 23% H1s (migrating hydrogen atom) and is the dominant orbital bonding the migrating hydrogen to the molecule. The 6a′ level is predominately a σ interaction between the C and O and has little electron density on the migrating hydrogen (see Supporting Information). The π_{CO} (1a″, out-of-plane) level is largely unperturbed by the migration of the hydrogen. In comparison to the formaldehyde, this level has 24% $C2p_x$ and 75% $O2p_x$, whereas the formaldehyde has 36% and 64%, respectively. This change decreases the double bond character of the transition state and thereby elongates the C−O bond (see Figure 13B). The transition state HOMO orbital, 7a′, resembles the HOMO of both the CH_2O in Figure 6 and the *trans*-HCOH in Figure 11. Its electronic structure is perturbed by the movement of the hydrogen atom, increasing the amount of $O2p_y$ (29%) at the expense of the C2s (19%) when compared to the *trans*-HCOH (see Supporting Information). Thus only the in-plane π level (5a′) bonds the migrating hydrogen to the HCO fragment. This bond is largely between the oxygen and the hydrogen atoms. Further geometry optimization of the transition state gives the formaldehyde molecule.

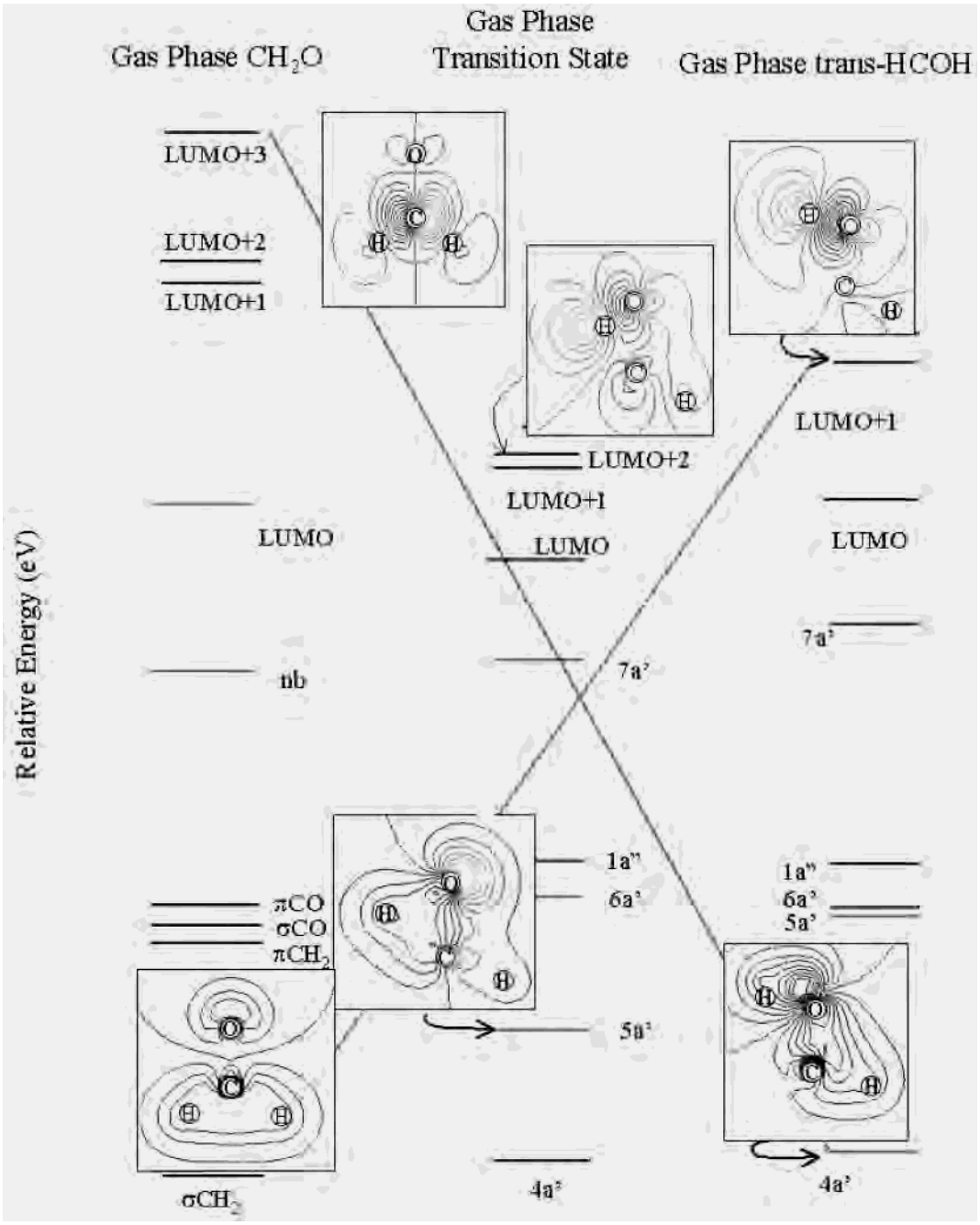

Figure 15. Gas phase energy level correlation diagram with the optimized gas phase CH_2O on the left, the gas phase transition state in the middle, and the optimized *trans*-HCOH on the right. The crossing of the CH_2O σ_{CH2} and the *trans*-HCOH 4a′ states is indicated with their correlating to the *trans*-HCOH LUMO + 1 and the CH_2O LUMO + 3 unoccupied levels, respectively. Electron density contours of the correlating levels and at the crossing point are shown. Energy scale has been aligned at the deepest level.

Schaefer et al.[37,108] in studies of the formaldehyde gas phase (*trans*-HCOH-to-CH_2O) rearrangement have attributed the barrier to a forbidden crossing reflected by a change in phase of the HOMO orbital of formaldehyde as the hydrogen migrates from the carbon to the oxygen end. An energy level correlation diagram of the change from formaldehyde through the calculated transition state to the *trans*-HCOH is presented in Figure 15. The energy level diagrams have been aligned at the deepest valence level. The origin of the barrier to rearrangement derives from those orbitals most affected by the forming and breaking of the C−H and O−H bonds. Focusing on the formaldehyde orbitals, the σ_{CH2} orbital is primarily the C−H bond and will become destabilized as the C−H hydrogen begins to migrate (Figure 15, left). On the *trans*-HCOH side of the correlation diagram (Figure 15, right), level 4a′ is the dominant interaction between the hydrogen and oxygen atoms. The energy of this level will be destabilized when the hydrogen begins to migrate.

On the formaldehyde side of the diagram (Figure 15, left), we note that a natural correlation exists between the σ_{CH2} (CH_2O) and the LUMO + 1 of the *trans*-HCOH (Figure 15, right). This unoccupied level maintains the formaldehyde σ_{CH2} phase and correlates levels that are dominated by the migrating hydrogen atom character. Similarly the *trans*-HCOH 4a′ level correlates with the high energy LUMO + 3 formaldehyde level (right-to-left upward

(108) Goddard, J. D.; Schaefer, H. F. *J. Chem. Phys.* **1978**, *70*, 5117.

Table 5. DFT Calculated Energy Levels of the HCOH Transition State on ZnO**(0001)**, Including Orbital Charge Decompositions

state	energy	% C	% O	% H	% H*	% Zn
in-plane π*	9.0	47	36	3	0	4% 3d, 3% 4p, 6% 4s
π out-of-plane	5.2	23	65	0	0	0
6a′	4.6	15	23	4	1	0
in-plane π	1.3	32	44	2	20	3% 3d, 4% 4s
4a′	0	41	14	30	0	0

rising line in Figure 15) as it maintains the hydrogen atom character and the proper phase relation between the hydrogen atoms. In addition this level has a nodal plane between the C and H atoms, similar to the *trans*-HCOH 4a′. These levels have the same a′ symmetry and undergo CI. Level 5a′ in the transition state is due to the bonding overlap of these two levels, which interact with the π_{CH2} (CH_2O) level (contour 5a′ in center of Figure 15). Its energy position has been stabilized by approximately 7 eV from the apparent crossing point.[109] The LUMO + 2 level of the transition state is the corresponding antibonding component of this interaction. The origin of the high energy barrier derives from the correlation and avoided crossing of these occupied and unoccupied molecular orbitals.

3.4.5. HCOH Transition State on ZnO. DFT calculations were next used to study the effect of the $Zn_{22}O_{22}$ cluster surface interaction with the transition state between HCOH and CH_2O. Starting with the surface bound *trans*-HCOH, a transition state calculation was performed. All atoms in the model, except the HCOH and the central Zn^{2+} ion, were constrained. The resulting transition state is shown in Figure 12B (HCOH fragment and the ZnO_3 site are shown). A vibrational calculation gave one imaginary frequency. The calculated surface bound transition state approximately resembles the gas phase, with the migrating hydrogen atom intermediate between the oxygen and carbon atoms. The HCOH transition state binds to the Zn^{2+} site with an O−C−Zn angle of 109.7° (see Figure 12B). However, the surface transition state obtained is not planar; the dihedral angle of the fragment is 23° (Figure 12B, inset). Importantly, the C−O bond has increased to 1.403 Å, from 1.325 Å in the gas phase calculation, indicating that a significant bond weakening has taken place. These geometrical changes, from the gas phase, impact the electronic structure and bonding of the transition state on the surface.

Figure 14 (right) presents the energy level diagram of the calculated surface transition state along with that of the gas phase. The energy of the deepest level, 4a′, has again been set to zero. Table 5 gives the atomic character of the calculated states. Two states are calculated to contain Zn character: the in-plane π*, with 4% 3d and 9% 4s, 4p Zn content, is similar to the 7a′ state in the gas phase, and the in-plane π with 3% 3d, 4% 4s, 4p Zn character is similar to the gas phase 5a′ state (Supporting Information). These states have been stabilized by their interaction with the Zn 4s, 4p by 0.6 eV and 0.4 eV, respectively. Their electron density contours in the plane that encompasses the Zn−C−H atoms are shown in Figure 14, right. A clear antibonding 3d component is observed along with an indication of an in-phase Zn 4p. The in-plane π contour (Figure 14, right, plane through Zn−C−O) provides a more direct visualization of the Zn−C bond. An in-phase bonding interaction is observed between the Zn^{2+} and the carbon atom. The stabilization of this state, through a bonding interaction with the Zn 4s, 4p, is due to its "bent" surface geometry. This geometry places the C−O bond, approximately, above the Zn^{2+}, enabling the oxygen atom to approach the Zn metal ion site more closely (2.77 Å). As discussed above, the in-plane π state (Figure 14, right) is stabilized by the interaction and mixing of the correlated states at the avoided crossing. Compared to the surface bound formaldehyde π_{CH2} level, the in-plane π contains an additional ∼2% Zn 4s, 4p character.

The increased total bonding interaction (total ∼13% Zn 4s, 4p) helps to stabilize the surface transition state and to facilitate the surface rearrangement of trans-HCOH to CH_2O. In comparison, the surface bound formaldehyde was calculated to have 6% Zn 4s, 4p and the trans-HCOH 5% Zn 4s, 4p content.

The geometry of the transition state indicates that the migration of the hydrogen atom and its concomitant geometry changes are facilitated and stabilized by its interaction with the surface. Thus, synchronous with the hydrogen migration is a rearrangement on the surface. At the transition state the C−O bond has been elongated and rotated to a Zn−C−O bond angle of 109.7°, a decrease of 25.5° from the surface bound *trans*-HCOH angle. The C−H and O−H bonds are similarly elongated (1.137 Å and 1.191 Å) as a consequence of the bonding interaction between the surface and the in-plane π molecular orbital. Along with this rotation is a translation of the surface species in an approximately parallel direction to the surface and toward the oxygen atom. The transition state bonding geometry is best described as pseudo η^2 (Figure 12B). Further geometry optimization of the transition state yields the oxygen end bound formaldehyde.

The increased bonding of the transition state to the ZnO surface translates into an overall stabilization of this species relative to the separated components. A calculation of the energy difference between the separated species on $Zn_{22}O_{22}$ and the observed surface bound transition state (Figure 12B) yields a stabilization energy of −26 kcal/mol. In comparison the *trans*-HCOH and CH_2O bonding interactions are considerably smaller, −19 kcal/mol and −15 kcal/mol, respectively, resulting in the greater relative stabilization of the transition state.

3.4.6. Methanol Synthesis Reaction Coordinate. The methanol synthesis reaction (MSR) on ZnO has been proposed to proceed through a surface bound formyl and through subsequent hydrogenation to yield CH_3OH.[28,110] The previous sections evaluated each step along this proposed reaction coordinate and have identified the probable overall transition state.

In order to facilitate the discussion of the proposed reaction coordinate on the ZnO surface, the gas phase reaction of $2H_2$ and CO to form CH_3OH is considered first (Figure 16, dashed line). These reaction steps will then be used to describe the reaction on the ZnO surface (vide infra), thus species 2 in the gas phase reaction corresponds to the 0 species on the surface. The energy of each species was calculated by computing the change in total energy from the separated constituents, which are then accumulated into a reaction mechanism in Figure 16. The specific gas phase species and steps are

$$\underset{(2)}{CO + 2H_2} \rightarrow \underset{(3)}{HCO^- + H^+ + H_2} \rightarrow \underset{(4)}{\textit{trans}\text{-HCOH} + H_2} \rightarrow$$

$$\underset{(5)}{\text{transition state} + H_2} \rightarrow \underset{(6)}{H_2CO + H_2} \rightarrow \underset{(7)}{H_3CO^- + H^+} \rightarrow \underset{(8)}{H_3COH}$$

The energy of step 2 → 3 is due to the difference between the breaking of the H_2 bond and the making of the H−CO bond (16 kcal/mol). A 20 kcal/mol increase in energy is observed at step 3 → 4, resulting from the formation of *trans*-HCOH, a known high

(109) Pearson, R. G. *Symmetry Rules For Chemical Reactions—Orbital Topology and Elementary Processes*; Wiley-Interscience: New York, 1976.

(110) Kung, H. H. *Catal. Rev.—Sci. Eng.* **1980**, *22*, 235.

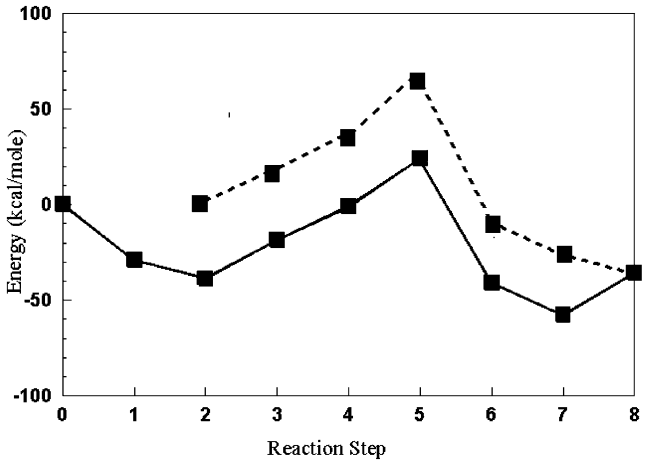

Figure 16. The change in calculated total energy of the gas phase (dashed line) and surface bound (solid line) methanol synthesis reaction. The description of the reaction steps is given in section 3.4.6 of the text.

energy intermediate. Step 4 → 5 is the gas phase rearrangement to the transition state. Step 5 → 6 completes the rearrangement of the transition state to formaldehyde. Step 6 → 7 is the formation of methoxide and an H^+, and step 7 → 8 adds the proton to the methoxide to form methanol. The calculated energy of the overall reaction is approximately −38 kcal/mol (experimental $\Delta H \sim -41$ kcal/mol).[111]

The solid curve in Figure 16 presents the reaction coordinate on the ZnO surface. The products identified along the abscissa in this figure are the following:

$$\underset{(0)}{3ZnO + 2H_2 + CO} \rightarrow \underset{(1)}{2ZnHOH + ZnO + CO} \rightarrow$$

$$\underset{(2)}{2ZnHOH + ZnO/CO} \rightarrow \underset{(3)}{ZnHOH + ZnOH + ZnO/HCO^-} \rightarrow$$

$$\underset{(4)}{ZnHOH + ZnO + ZnO/\textit{trans}\text{-}HCOH} \rightarrow$$

$$\underset{(5)}{ZnHOH + ZnO + ZnO/\text{transition state}} \rightarrow$$

$$\underset{(6)}{ZnHOH + ZnO + ZnO/CH_2O} \rightarrow$$

$$\underset{(7)}{ZnOH + ZnO + ZnO/CH_3O^-} \rightarrow \underset{(8)}{3ZnO + CH_3OH}$$

The first step in the reaction, step 0 → 1, is the binding of $2H_2$ molecules and is twice the calculated heat of adsorption or −30 kcal/mol as protons on the oxide and hydrides on the zinc(II). Step 1 → 2 is the interaction of CO with the surface (−9 kcal/mol). Step 2 → 3 is the formation of formyl by hydride attack at the carbon atom of the bound CO. Step 3 → 4 represents the proton attack on the formyl anion. The hydrogen migration and ultimately the surface rearrangement of the *trans*-HCOH to CH_2O proceeds through the calculated transition state (see section 3.4.5), given in step 4 → 5. It is also the highest energy barrier in this reaction coordinate. The interaction with ZnO leads to a greater relative stabilization of the transition state on the surface, which is reflected in the lower rearrangement barrier height on the surface compared to the gas phase (∼22 kcal/mol versus ∼31 kcal/mol, Figure 16).

The subsequent rearrangement of the transition state to the η^1 bonded, oxygen end bound, formaldehyde is given in step 5 → 6.

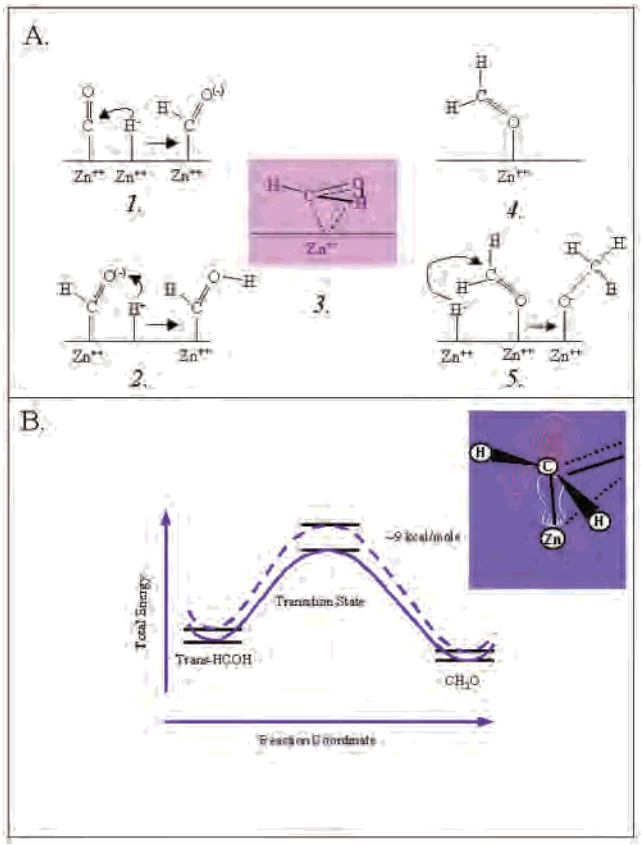

Figure 17. (A) Schematic of the MSR reaction on the ZnO surface. (B) Diagram of the greater relative stabilization of the surface bound transition state compared to the gas phase and surface bound CH_2O and *trans*-HCOH. Inset gives the contour of the principal transition state bonding orbital the in-plane π.

The energy of this step (∼-62 kcal/mol) is reduced when compared to the gas phase reaction (∼−82 kcal/mol). Thus the transition state is stabilized most by its interaction with the surface, when compared to the *trans*-HCOH and CH_2O interactions. From Figure 16, both the forward and back reaction barriers at the transition state are less than in the gas phase. Step 6 → 7 envisions the hydride attack at the carbon atom forming bound methoxide. In step 7 → 8 the transfer of an H^+ to the methoxide yields gas phase methanol (see Figure 16, solid line). The overall energy of this surface reaction is negative, indicating an exothermic reaction. The experimental enthalpy of formation of methanol is −41 kcal/mol,[111] in reasonable agreement with the calculated value (−38 kcal/mol).

4. Discussion

The MSR reaction over ZnO is thought to begin with the activation of surface bound carbon monoxide for hydride attack forming the formyl intermediate.[28] Previous experimental results from this laboratory have elucidated the geometry and electronic structure of CO bound to the ZnO-**(0001)** and ZnO**(10$\bar{1}$0)** surfaces.[23] A net positive charge on the carbon atom was determined, which activates it for hydride attack.[99] DFT geometry optimized calculations in the present study indicate that the hydride necessary for this surface reaction can derive from the heterolytic cleavage of H_2 over the ZnO**(0001)** surface. Figure 17A, step 1 highlights this attack on the surface.

The formyl intermediate has been observed on the ZnO-**(0001)** surface (C1s XPS peak position 291.5 eV, Figure 7A)

(111) Hine, J.; Arata, K. *Bull. Chem. Soc. Jpn.* **1976**, *49*, 3089.

after low temperature annealing. This important intermediate in the Costa−Muetterties reaction scheme has been previously observed at 220 K on the ZnO surface with FT-IR spectroscopy[86−88] and as the decomposition product of methanol on Rh(111) and Rh(111)−(2×2)O surfaces[112] in this same temperature range.

The experimental observation of a surface formyl is an important result of the current study. Its subsequent reactivity was probed with DFT and frontier molecular orbital theory (FMO). The DFT calculations show that the oxygen atom has a large negative charge and the largest coefficient in the HOMO (Table 3), indicating that the expected position of proton attack will be the oxygen atom of the HCO^- surface intermediate. A schematic of the reaction of the surface intermediate is portrayed in Figure 17A, step 2. Thus, consistent with experiment, surface bound formyl is calculated to be η^1 bonded to the Zn^{2+} site and activated for H^+ attack at its oxygen atom.

This study has used a combination of experimental and computational techniques to describe the bonding of formaldehyde on the ZnO surface. One C1s XPS peak is observed when CH_2O is bound to the surface. Its energy position (292.7 eV IP), when corrected for relaxation, is consistent with a small positive increase in charge at the carbon atom. However, no change in the C−O bond length is observed by NEXAFS spectroscopy upon bonding to the surface. Variable energy PES spectra indicate that two formaldehyde orbitals are principally involved in bonding to the surface Zn^{2+} site (π_{CH2} and nb, Figure 3). In contrast, η^2 bound aldehydic compounds typically have shake-up structure in their C1s XPS spectra due to the involvement of the π^* orbital that is centered on the C−O bond;[23,113] they have increased net negative charge on the carbon atom and elongated C−O bonds.[114] These experimental observations show that CH_2O bonds to ZnO in an η^1 geometry with no back-bonding (Figure 17A, step 4). Similar η^1 bound formaldehyde surface intermediates have been observed on oxygen dosed Pd(111) surfaces[115] and on Rh(111) and Rh(111)−(2×2)O surfaces.[112] It is important to note that the observation of an oxygen bound formaldehyde derived from the protonation of the carbon end bound formyl species requires both an inter- and intramolecular rearrangement.

DFT calculations show that after attack of the surface HCO^-, by a proton at the oxygen atom, the resulting trans hydrogen isomer of formaldehyde would be the more stable on the surface (Figure 17A step 2). The carbon end bound *trans*-HCOH is planar and orientated to facilitate a rearrangement on the surface (Figure 12A). The gas phase rearrangement of this species to CH_2O was probed with DFT. A transition state search indicated that this reaction proceeds with a high barrier (Figure 13D) due to the avoided crossing of levels in the correlation between the *trans*-HCOH and CH_2O gas phase species. At the crossing point they interact (solid line),[116] thereby lowering the barrier. However, a significant barrier remains, which is responsible for the observed transition state. This barrier is decreased when the transition state is bound to the surface due to a stabilizing interaction of the orbital derived from the avoided crossing with the 4s and 4p orbitals in the Zn^{2+} site. Figure 17B presents a comparison of the gas phase and surface bound barrier in diagrammatic form. The rearrangement (Figure 17B) on the ZnO**(0001)** surface exhibits a barrier to reaction that is 9 kcal/mol lower than the gas phase. Unlike the gas phase, the geometry of the calculated surface transition state is not planar (Figure 17A, step 3). This change in geometry is due to an additional interaction with the Zn^{2+} site that facilitates the reorientation to surface bound CH_2O. The resulting η^1 CH_2O is stabilized on the surface by a bonding interaction with the unoccupied Zn 4s and 4p levels (Figure 6C,D, Table 2).

The formation of methoxide is energetically downhill from formaldehyde. The DFT geometry optimized calculations show that methoxide is η^1 oxygen end bound to the ZnO-**(0001)** surface (Figure 17A, step 5). This is consistent with our previous C1s XPS and NEXAFS study identifying methoxide on the ZnO surface from its interaction of methanol.[24]

The MSR reaction over ZnO takes place with a barrier of approximately 27 kcal/mol (ΔG). In section 3.4.5 we examined the MSR reaction starting with CO on the ZnO surface and correlated the reaction barrier with the transition state in the rearrangement of the *trans*-HCOH to formaldehyde (Figure 12B). The barrier given in Figure 16 was derived from the change in total electronic energy for this reaction and therefore does not include entropy or zero point energy corrections. In order to compare the calculated and experimentally determined barriers it is necessary to include vibrational effects in this calculation. To accomplish this, vibrational calculations were undertaken on small cluster models of the adsorbed species (see Supporting Information) interacting with the central Zn(II) site. These small clusters were derived from the $Zn(O)_3$ C_{3v} site and included one proton on each oxide (i.e. $Zn(OH)_3^{(-1)}$).[33] The *trans*-HCOH surface species was optimized on this small cluster (with the cluster geometry frozen) and yielded a geometry in reasonable agreement with that found with the larger $Zn_{22}O_{22}$ cluster ($Zn(OH)_3^{(-1)}$−CHOH, Zn−C 2.03 Å and C−O 1.38 Å, see Figure 12A). The previously determined transition state geometry was used to start the transition state search on the smaller cluster. The transition state obtained on the small cluster ($Zn(OH)_3^{(-1)}$) is also in reasonable agreement with the species found on the larger cluster (Zn−C 1.88 Å and C−O 1.37 Å, see Figure 12B).

The thermodynamic properties derived from these smaller geometric models are given in the Supporting Information. This table includes results from both the calculated gas phase rearrangement and this reaction on the $Zn(OH)_3^{(-1)}$ cluster. ΔD_e denotes the change in total electronic energy (transition

(112) Houtman, C.; Barteau, M. A. *Langmuir* **1990**, *6*, 1558−1566.
(113) Didziulis, S. V.; Cohen, S. L.; Butcher, K. D.; Gewirth, A. A.; Solomon, E. I. *J. Am. Chem. Soc.* **1988**, *110*, 250.
(114) Tsou, T. T.; Huffman, J. C.; Kochi, J. K. *Inorg. Chem.* **1979**, *18*, 2311.
(115) Davis, J. L.; Barteau, M. A. *Surf. Sci.* **1992**, *268*, 11−24.
(116) Albright, T. A.; Burdett, J. K.; Whangbo, M. H. *Orbital Interactions In Chemistry*; Wiley-Interscience: New York, 1985.

state − *trans*-HCOH). It should be noted that the change of electronic energy on the small cluster is very similar to that calculated using the larger cluster (section 3.4.5). ΔE_{vib} is the contribution to the total energy due to the change in the vibrational modes (transition state − *trans*-HCOH) and includes the zero point vibrational correction. A comparison of ΔE_{vib} in the gas phase and on the surface shows them to be similar, implying that there is no significant change in vibrational energy when bound to the surface. The calculated entropic contribution, $T\Delta S$ (at $T = 298$ K), for the gas phase and on the surface is less than 1 kcal/mol (see Supporting Information). The small size of this contribution to ΔG reflects the fact that no bonds are broken in the reaction. The calculated change in entropy for the surface reaction is negative, which is consistent with a more tightly bound surface species in the transition state. The calculated ΔG for the surface reaction is 26.5 kcal/mol, which is approximately 8 kcal/mol less than in the gas phase. It is dominated by the electronic energy contribution, which indicates that the calculated barrier in Figure 16 is a reasonable approximation to the total energy path from the *trans*-HCOH to the transition state on the surface.

A final aspect of this study is the observation of different temperature dependent surface chemistry on the two chemically different surfaces of ZnO. A rich temperature dependent chemistry is observed on the **(0001)** surface. Formyl, formate, and methoxide are all formed on this surface. However, no formyl or methoxide are formed on the **(10$\bar{1}$0)** surface. This difference has consequences for the MSR reaction over ZnO. Kung et al.[30] have shown that only the **(0001)** surface is active in methanol synthesis. Our previous results on the surface dependent reactivity of methoxide have shown that no reaction takes place on the ZnO**(10$\bar{1}$0)** surface whereas formate is formed on the **(0001)** surface. The lack of reaction of the methoxide was attributed to structural differences between these two surfaces.[24] A formaldehyde intermediate was suggested as necessary for the formation of formate. This is confirmed by the current study with the observation of the formation of formate from formaldehyde on the **(10$\bar{1}$0)** surface. The fact that the MSR activity of the **(10$\bar{1}$0)** surface is extremely low and that CH_2O would produce formate on this surface indicates that in contrast to past proposals the decomposition reaction of formaldehyde to formate is not an important reaction pathway in methanol synthesis over ZnO.

Acknowledgment. Support for the work performed at the Stanford Synchrotron Radiation Laboratory, which is operated by the U.S. Department of Energy, Office of Basic Energy Sciences, is greatly acknowledged.

Supporting Information Available: Full experimental descriptions and listings of Cartesian coordinates for all optimized and transition state structures. Figure of ZnO cluster model and table of charges on adsorbed species. Tables of molecular orbital charge decompositions and the ZnO cluster structure and table of thermodynamic properties. This material is available free of charge via the Internet at http://pubs.acs.org.

IC035252Q